A Novel Thiolated Hyaluronic acid Hydrogel for Spinal Cord Injury Repair

Ruifu Li

A thesis submitted to the

Faculty of Graduate and Postdoctoral Studies

In partial fulfillment of the requirements

For the MASc degree in Chemical Engineering

Department of Chemical and Biological Engineering

Faculty of Engineering

University of Ottawa,

Acknowledgments

I would like to extend my sincerest thanks and appreciation to my supervisor Dr. Xudong Cao, for his patience, background knowledge, guidance and support over the course of this research. He was a constant inspiration, and his assistance and suggestions were invaluable towards the completion of this work.

I would also like to thank Dr. Erik Suuronen and Donna Padavan for granting access to the rheometer, and the help in rheological experiment. To the other members of my group, especially Yan Du, Chunyu Lu and Jian Tang, thank you for the assistance when I needed it.

Finally, I would like to express my deepest gratitude to my parents, for their support, patience and encouragement during my pursuit of the Master's degree.

Table of contents

List of Figures

List of Schemes and Tables

Abstract

Spinal Cord Injury (SCI) often causes cell death, demyelination, axonal degeneration and cavitation, resulting in functional motor and sensory loss below the site of injury. In an attempt to overcome SCI, the regenerating neurons require a permissive environment to promote their ability to reconnect. We report a novel thiolated hyaluronic acid (HA) hydrogel scaffold that can be used to repair the injured spinal cord. More specifically, thiolated hyaluronic acid hydrogels with varying thiol concentrations were successfully synthesized. The amount of thiol groups was measured spectrophotometrically using Ellman's test. HA gels with different crosslinking densities were synthesized and the water content of the hydrogels was determined. The thermal behavior of the HA gels were studied by DSC. The strength of the hydrogels with varying thiol group content was evaluated by a rheometer. In addition, *in vitro* enzymatic degradation was performed through submerge the hydrogels in 200U/ml of hyaluronidase solution and incubate at 37°C. According to the result of the present study, this novel hydrogel shows great potential to serve as a 3D cell-patterning scaffold which can be inserted into a hollow fiber channel that could be used to promote regeneration after the SCI.

Résumé

La lésion de la moelle épinière provoque souvent la mort des cellules, démyélinisation, une dégénérescence axonale et la cavitation, qui se résultent dans le moteur fonctionnelle et une perte sensorielle situer en-dessous de la blessure. Dans une tentative pour surmonter les blessures d'une lésion de la moelle épinière, les neurones de régénération nécessitent un environnement permissif pour favoriser leur capacité de se reconnecter. Nous rapportons un nouveau thiolée d'acide hyaluronique (AH) hydrogel d'échafaudage, qui peut être utilisé pour réparer la moelle épinière qui est blessée. Plus précisément, l'acide hyaluronique thiolées hydrogels avec des concentrations variables de thiol ont été synthétisés avec succès. La quantité de groupe de thiol a été mesurée par spectrophotométrie en utilisant le test d'Ellman. Les gels AH avec différentes densités de réticulation ont été synthétisés de la teneur en eau des hydrogels ont été déterminée. Le comportement thermique des gels AH ont été étudiées par DSC. La résistance des hydrogels avec des teneurs variables en groupes de thiol a été évaluée par un rhéomètre. En outre, in vitro, la dégradation enzymatique a été effectuée à travers les hydrogels immergés dans 200U/ml de solution de hyaluronidase et incubé à 37°C. Selon le résultat de l'étude présent, ce nouvel hydrogel a montré un grand potentiel pour servir comme une image de trois dimensions d'une cellule échafaudé de motif qui peut être inséré dans un canal de fibre creux qui pourrait être utilisé pour favoriser la régénération après une blessure de la lésion de la moelle épinière.

Nomenclature

ATR	attenuated total reflectance
BDNF	brain-derived neurotrophic factor
$BM(PEG)_2$	bismaleimide-activated polyethylene glycol
cAMP	cyclic adenosine monophosphate
CNS	central nervous system
CSPG	chondroitin sulfate proteoglycan
ddH_2O	deionized distilled water
DSC	differential scanning calorimetry
DTNB	5,5'-dithiobis-(2-nitrobenzoic acid)
DTT	dithiotheitol
EDC	1-(3-dimethylaminopropyl)-3-ethyl-carbodiimide
EDTA	ethylenediaminetetraacetic acid
ECM	extracellular matrix
FGF	fibroblast growth factor
FT-IR	Fourier transform infrared
GAG	glycosaminoglycan
GF	growth factor
GlcNAc	β-1,3-acetyl-D- glucosamine
GlcUA	α-1,4-D-glucuronic acid
HA	hyaluronic acid
HAase	hyaluronidase
IKVAV	lle-Lys-Val-Ala-Val

Mag	myelin-associated glycoprotein
MVC	motor vehicle collision
NGF	nerve growth factor
NHS	N-hydroxylsuccinimide
Omgp	oligodendrocyte myelin glycoprotein
PEG	polyethylene glycol
PNS	peripheral nerves system
PVP	poly(N-vinyl-2-pyrrolidone)
REDV	Arg-Glu-Asp-Val
RGDS	Arg-Gly-Asp-Ser
RGM	repulsive guidance molecule
RHAMM	receptor for hyaluronic acid mediated motility
SCI	spinal cord injury
TSCI	traumatic spinal cord injury
UV	ultraviolet
YIGSR	Tyr-lle-Gly-Ser-Arg
3D	three-dimensional

1. Introduction

Natural or synthetic materials which are suitable for introducing into living tissue are generally known as biomaterials [1]. Synthetic materials can be synthesized through some chemical methods utilizing metals, polymers, ceramics or composite materials. Biomaterials in the form of implants (bone plates, heart valves, dental implants, vascular grafts, sutures, ligaments, intraocular lenses, joint replacements, etc.) and medical devices (biosensors, pacemakers and artificial blood vessels tubes to name a few) are often used to substitute whole or part of a living structure or a bio-device which performs or replaces a natural function, to enhance survival or improve quality of life [2].

Nowadays, injuries to the central nervous system (CNS) are characterized by the inability of the injured axons to regenerate. No functional recovery method exists, particularly for the patients who have spinal cord injuries (SCI). Although palliative care services are available to improve the quality of patients' life, there is still no effective way to restore motor, sensory, and autonomic functions. The SCI usually makes patients permanently injured. A therapy to help overcome SCI would need to both provide new neurons or neural stems cells to the affected area, and stimulate and direct their growth so that they can form the correct connections with other neurons and restore proper functions. Our ultimate goal is to develop a novel hydrogel for three-dimensional patterns to enable nerve regeneration after SCI.

1.1 A short history of biomaterials

The use of biomaterials dates back to ancient civilizations. Two thousand years ago, it was found gold was used in dental applications in China, Rome and by the Aztec. Glass eyes and wooden teeth were recorded next. Synthetic plastics were developed in the turn of the last century. Just after World War II, vascular prostheses were made with parachute cloth. However, the word “biomaterial” had not appeared when these applications had already spanned much of the written history. However, the origin of the term “biomaterials” was probably invoked through the early Clemson University biomaterials symposia in the late 1960s and early 1970s. It led to the formation of the Society for Biomaterials in 1975 [3].

The development of biomaterials has been an evolving process. Polymeric materials, as a type of biomaterials have unique chemical structures which can provide specific functions for desired applications, and have great impact on the improvement of health and quality of life. There has been extensive research on polymeric materials over the past several decades. The integration and multipurpose usages of polymer biomaterials depend on the advances in the synthesis of polymers with controlled methods and functional architectures, which can enhance their biocompatibility[4] [5]. According to their different effects on organisms, polymeric biomaterials can be divided into two main parts: non-biodegradable (bio-inert materials) and biodegradable polymeric materials.

1.2 Biodegradable polymeric materials

As the widely used polymeric biomaterials, non-biodegradable polymers, such as polyethylene, nylon and silicone rubbers, have some key properties: biostability, implantability, chemical resistance and ease of sterilization [6]. With the recent development in the field of tissue engineering, regenerative medicine and drug controlled release, biodegradable polymers have started playing a major role and have become a new research frontier.

Biodegradable polymeric materials are defined as polymers which are bio- and environmentally degradable. Figure 1.1 shows different types of polymer degradations. Hydrolysis and enzymatic cleavage are the main reasons leading to a scission of the polymer backbone which can cause degradation. The advantages of biodegradable polymers are the following [7-11]:

- Their degradation does not lead to inflammatory or toxic response;
- They are metabolizable in the body after they complete their purpose, leaving no trace and avoiding a second surgical intervention for removal;
- With the polymeric materials' degradation, the surrounding tissue is continuously repaired and then healed;
- They offer tremendous potential as the basis for controlled drug delivery because they can release drugs gradually.

In terms of sources, there are two general types of biodegradable polymers: natural biodegradable polymers and synthetic biodegradable polymer materials. These polymer materials are extremely useful for various applications in many fields currently, such as medical, drug release and packaging, etc. In this study, we used

natural biodegradation material, including alginate [12, 13], chitin and chitosan [14-16], starch, hyaluronan [17-20], and gelatin [21, 22].

Hyaluronic acid (HA) was chosen for the fabrication of hydrogels in our study. HA is a naturally occurring component of the extracellular matrix (ECM) and is found in synovial fluid, connective tissues and organs of all higher animals [4, 23-25]. More details of HA will be reviewed in the next section (Literature review). Generally, HA is an ideal choice for the pattern base because (i) it is a component of the natural cell microenvironment and known to support cell proliferation [26], (ii) it naturally shows cell anti-adhesive properties in that it prevents the background binding of cells located off-pattern [27], and (iii) it has the reactive carboxyl groups that can be used for chemical crosslinking to form stable hydrogels [17, 20, 28]. Although pure HA has a high degradation rate in vivo, it can also be chemically modified to alter its properties by esterification [29], cross-linking [17, 20], and binding with other polymers [30]. For example, one method consist in attaching thiol groups to HA, then using the thiol groups to crosslink and form the hydrogel has been reported [20, 23, 31].

Type I

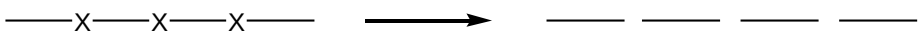

X represents the labile backbone bonds

Type II

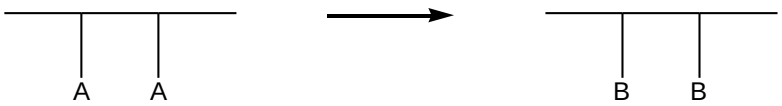

A represents hydrophobic side group

B represents hydrophilic side group

Type III

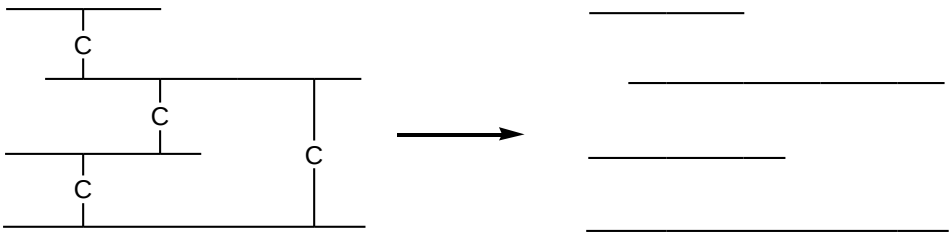

C represents the crosslinks

Figure 1.1 Different types of polymer degradation.

2. Literature survey

2.1 Spinal cord injury

2.1.1 Overview of SCI

Spinal cord is a tubular bundle nervous tissue that can be classified into five sections: the cervical, thoracic, lumbar, sacral, and coccygeal regions [32]. Traumatic injury to spinal cord is an annihilating disorder of the central nervous system and often leads to devastating personal, economic and social problems. The current reality is that the mammalian CNS is unable to fully regain function after injury, the clinical consequences of which are often permanent loss of sensory, motor, and autonomic functions. Over the past few decades, young males have been known to be at the highest risk for traumatic SCI (TSCI), mainly caused by motor vehicle collisions (MVC) [33, 34]. A cohort study of TSCI in Canada has been done by Pickett *et al.* [35], in which TSCI was investigated by fitting a bimodal distribution by age. Groups that have higher risk of traumatic SCI include not only young males, but also elders more than 60 years old. Falls are another cause of spinal cord injury. Noonan *et al.*[36] also estimated initial incidence of traumatic SCI is 1,785 cases per year, and the discharge incidence is 1,389 (41 per million) in Canada in 2010. Moreover, the direct costs of healthcare in the traumatic SCI population were estimated to range between $100,000-$130,000 Canadian Dollars (CAD) per person. In-patient rehabilitation care is the largest cost in the health care system [37]. It is life changing for the injured people and their family, and also has horrendous social costs for health care treatment, recovery, loss of productivity, to name a few [38].

2.1.2 Inhibitory factors

In mammals, two main obstacles prevent neural regeneration: inhibitors present within myelin and the formation of a glial scar. After CNS injury, oligodendrocyte precursors, microglia, meningeal cells, astrocytes, etc., are assembled to the site. Axon growth inhibitory molecules associated with myelin and the glial scar prevent axon regeneration by acting as a barrier at the injury site to inhibit axon growth *in vivo*, and result in permanent loss of motor, sensory, and autonomic function below the area of injury [39-41].

2.1.2.1 Inhibitors of regeneration in myelin

Interestingly, myelin extracted from peripheral nerves system (PNS) was shown to be growth permissive whereas CNS myelin strongly inhibited nerve growth. As first described by Ramon y Cajal, white matter could 'block' regeneration in the CNS [42]. But it was no longer true till Schwab and his colleagues did their research in the late 1980s and gave a molecular insight into the mechanism of inhibition [43, 44]. The IN-1 monoclonal antibody, which could help neurite extension, allowed axons to grow on myelin both *in vitro* and *in vivo* [44, 45]. The antigen for the IN-1 antibody was identified after a decade. Three groups independently cloned an antigen of the IN-1 antibody, which was named Nogo by Schwab [46, 47]. In addition, multiple components of CNS myelin that inhibit axonal growth were identified by investigators, such as myelin-associated glycoprotein (Mag)[48, 49], oligodendrocyte myelin glycoprotein (Omgp)[50], repulsive guidance molecule (RGM)[51] and ephrin-B3 [52].

A therapy that emerged from research was the use of the IN-1 anti-Nogo antibodies. This work was initiated over two decades ago, directed against what was then known as 2 neurite outgrowth inhibitors, NI-250 and NI-35 (i.e. Nogo)[44]. Schnell et al. indicated that the IN-1 antibody in a partial transection model of SCI in the rat was found to promote axonal regeneration after injury [53] and functional recovery [54]. The anti-Nogo antibody treatment strategy has been commercialized by Novartis, as one of the most promising approaches to enhance axonal regeneration following SCI. But one obvious question about the use of antibody treatments (or other myelin inhibitors) is the functionality of the axonal sprouting that might be induced. Myelin-associated inhibitors may have evolved as means to maintain the structural integrity of synaptic networks formed during development and limit sprouting following developmental pruning and myelination.

2.1.2.2 Glial scar–associated inhibitors

Glial scar formation is a reactive cellular process which can cause reactive astrogliosis after injury to the CNS. The place where regeneration of axons fails necessarily contains a glial scar. All the five cell types, astrocytes, oligodendrocyte precursors, oligodendrocytes, microglia, and meningeal cells have inhibitory properties, which mean any one kind of these cells is potentially sufficient to block regeneration of most CNS axons.

The cells that comprise the glial scar secrete some growth inhibitory extracellular matrix components, known as chondroitin sulfate proteoglycans (CSPGs) which inhibit axonal outgrowth [55, 56]. The CSPGs (neurocan, brevican, versican, aggrecan, phosphacan and NG_2 [57]) have a protein core which attach sulfated

glycosaminoglycan (GAG) chains through covalent bond. *In vitro* studies demonstrate that the ability of CSPGs restricts neurite outgrowth from various kinds of cultured neurons and indicates inhibitory properties owing to the chondroitin side chains on CSPGs [58-60]. Moreover, increased levels of CSPGs present in the area wound inhibit axon regeneration. For this reason, various treatments have attempted to eliminate the chemical components of the glial scar or adjust their negative effects, especially by eliminating the CSPGs [61, 62].

2.1.3 Nerve growth factor

Growth factors (GFs) are naturally occurring substances which are defined as protein or steroid hormone [63]. They are capable of stimulating neurite outgrowth, cell survival, proliferation in the case of cells capable of mitosis, and differentiation in biological environment. GFs have different cell type specifications; some GFs (e.g., nerve growth factor) stimulate only one or few cell types while others (e.g., insulin-like growth factor) stimulate a wide variety of cell types. Over the past several decades, the number of growth factors has continually increased and been grouped as members of some 'families'. Nerve growth factor (NGF) denotes a heterogeneous group of neurotrophic agents, which were discovered and characterized by Levi-Montalcini and Cohen [64]. NGF participates in a wide range of actions in adult animal, such as axon growth, peptides synthesis, transmitter enzymes and calcium-binding proteins, dendritic arborization, sprouting and myelination [65]. For these reasons, it can be expected that NGF will enhance axonal regeneration [66-68].

2.1.4 Development of neurotrophic factors therapeutic methods

The preceding section highlights the fact that nerve growth factor can arouse growth of axon and promote functional recovery in the injured spinal cord [69]. In addition, other neurotrophic factors have beneficial effects on different kinds of axons. For example, NT-3 promotes growth of corticospinal axons [70]; Brain-derived neurotrophic factor (BDNF) can boost rubrospinal and propriospinal axon growth [71] and acidic fibroblast growth factor (FGF) has been reported to promote the regeneration of supraspinal axonal projections in the spinal cord [72]. But several problems inhibit the translation of these promising discoveries from animal models of spinal cord injury to the clinical application [73]:

a. Suitable scaffolds must provide structural support to the injured spinal cord over which injured axons can extend.
b. The mechanisms of function restored in rodent models of spinal cord injury need to be understood to then predict which factors are worth to test in humans with spinal cord injury.
c. The differences between the rodent models and human spinal cord were required to be tested before clinical trials can be justified in humans, such as spinal cord organizations, projection patterns and functions exist.

As mentioned above, neurotrophic factors have the potential to regenerate the motor neurons at the level of a spinal cord injury. However, comparing with other single therapies, such as cellular replacement and neutralization of myelin-associated inhibitors, they all remain the subject of continued debate so that their applications are extremely limited.

Over the past decade, some groups published several inspiring papers, reporting that combinations of treatment approaches exert greater effects on axon regeneration than single therapies [74, 75]. For example, in order to realize the regeneration of dorsal column sensory axons into and beyond the lesion site, combinatorial therapies can support both intrinsic and extrinsic neuronal growth. Intrinsic mechanisms were achieved by increasing the level of cyclic adenosine monophosphate (cAMP) in sensory neuronal soma; extrinsic mechanisms were targeted by placing extra- and intra-cellular matrices in the lesion site to lead axonal attachment and by dosing neurotrophic factors within and beyond the bridge in lesion site to provide a trophic stimulus to injured axons [67]. Houle et al. also confirmed that combinatorial therapies can enhance the axon regeneration in rodent models of spinal cord injury [76]. Furthermore, truly axonal regeneration is difficult to achieve because it requires targeting both intrinsic and extrinsic mechanisms through different therapies to achieve limited numbers and distances of regenerating axons. It may be difficult for just one therapy to handle this complicated issue. Although some practical obstacles to combinations of treatment approaches need to be overcome, such as design a combinatorial approach in larger animal models instead of rodent models, it still may bring benefits to humans at last.

2.2 Hydrogels

Pharmaceutical chemistry has developed steadily in recent years and has become invaluable in helping people prevent disease and keep healthy. In the past few decades, research in the treatment of diseases via biomolecules, such as drugs and proteins, has progressed a lot. Initially, biomolecules could just be administered in limited ways, due to some of the restrictions of drug delivery in the body [77]. And then, biomaterial carriers, which can be encapsulated or immobilized with drugs, are discovered, allowing the drugs reach the required site safely. These carriers realized the drugs release in the location which was inaccessible formerly. After years of evolution, the nature of these carriers has progressed from ceramics to synthetic materials [78]. Many factors were considered during the design process of the carriers, such as integrity, biocompatibility and flexibility. This has led to the use of hydrophilic three dimensional matrices as carrier materials. This class of materials is known as hydrogels. Synthetic hydrogels can be prepared from varied monomers, and has many applications, especially in tissue engineering. They provide an effective and controlled way in which to administer proteins and peptides for treatment, because hydrogels have ordered polymer networks and physicochemical properties [77]. Therefore, hydrogels have become a premier material used for drug delivery and biomedical implant devices.

2.2.1 Properties of hydrogels

Hydrogels are hydrophilic and highly absorbent polymer matrices, capable of imbibing a great deal of water or biological fluids when placed in aqueous environment [79, 80]. Their high water content and soft consistency contribute to

their biocompatibility. These gels resemble natural living tissue more than any other kind of synthetic biomaterial, making them ideal materials for applications in tissue engineering [81]. The hydrogel networks, which have a three dimensional structure and are composed of homopolymers or heteropolymers, can be split into 'physical' (e.g., entanglements, crystallites) and 'chemical' gels (tie-points, junctions) [82, 83]. Physical hydrogels' network formation is reversible. In contrast, chemical crosslinks are established by irreversible covalent bonds. Combinations of both physical and chemical networks can also be achieved, e.g. gelatin modified with methacrylamide groups [84]. As mentioned above, the biocompatibility and crosslinked structure of hydrogel make them usable for contact lenses, artificial skin, membranes for biosensors and drug delivery devices [5, 85, 86].

2.2.1.1 Water swollen capacity and absorption capacity

The water swollen capacity and absorption capacity both are important properties of the hydrogels that bring them wide applications. The presence of polar hydrophilic groups, such as –OH,-COOH and $–CONH_2$- in the network, bound with the water molecules and affect the swelling and absorption properties [87]. The network will intake additional water due to the osmotic driving force [88]. This additional swelling is opposed by the chemical or physical crosslinks, leading to an elastic retraction force in the network. Then, the hydrogel will reach equilibrium.

2.2.1.2 Biocompatible properties

Biocompatibility is important for hydrogels as useful biomedical polymers. It relates to the material's ability to exist within the body without damaging cells or resulting in significant scarring or eliciting an opposite response from desired function [89].

Most polymers used for biomedical applications must have cytotoxicity assays and in-vivo toxicity tests. Most toxicity problems associated with hydrogels arise from the unreacted monomers, oligomers and initiators. Thus, an assessment of the potential toxicity of a material used in hydrogel fabrication is a necessary part of the determination for biological applications. In order to decrease toxic effects, gamma irradiation is employed as polymerization technique instead of the use of initiators [90]. Steps are taken to remove impurities from hydrogels by repeated washing and immersing. The kinetics of polymerization has also been studied to achieve higher conversion rates, and avoid unreacted monomers and byproducts.

2.2.1.3 Mechanical properties

The mechanical properties of hydrogels are essential design parameters in tissue engineering, because the gel must maintain physical and mechanical integrity and create a space for tissue development. In addition, the adhesion and gene expression of cells have strong correlation with the mechanical properties of the polymer scaffold [91]. Typically, the crosslinking molecules' type, the original rigidity of polymer chains and the crosslinking density determine the mechanical properties of hydrogels [92]. The strength of the hydrogel can be increased by adding crosslinkers and monomers to increase the degree of crosslinking. However, there is an optimum degree of crosslinking. A higher degree of crosslinking leads to more brittleness and less elasticity. Elasticity is also an important parameter for hydrogels. It means flexibility for the crosslinked chains, and capability to stimulate movement of incorporated bioactive agent. Thus, it is necessary to find a balance between mechanical strength and flexibility for hydrogels' applications.

2.2.1.4 Controlled degradation

It is important to control the degradation rate of hydrogels in tissue engineering, whether the gels are obtained from natural or synthetic substances. Typically, the degradation rate of a scaffold and the time of tissue development need to be considered and will depend on the type of tissue to be engineered. Many reasons can cause hydrogels' degradation, such as hydrolysis, enzymatic action and dissolution [89]. The degradation rates of crosslinked gels can affect the mechanical properties by introducing network defects, and resulting in the formation of soft hydrogels with longer degradation time than for high crosslinked gels [93].

2.2.2 Preparation of hydrogels

Hydrogels are crosslinked polymeric networks which can swell in water or biological fluids [86]. They can be used for release control and for cell or biomolecule encapsulation. In most cases, the polymer structure of hydrogels can degrade in no potential toxic products [3]. The preparation methods of hydrogels include chemical and physical crosslinking, both of which are used for the design of biocompatible hydrogels and will be discussed in detail. In this study, the hydrogels were crosslinked via crosslinking agent BM$(PEG)_2$, which can form covalent bonds and ensure hydrogels to be mechanically stable.

Physical crosslinks are entanglements, crystallites, and association bonds such as hydrogen bonds and strong van der Waals interactions [77]. The physical gels can be classified as strong physical gels and weak physical gels. Strong physical gels have strong physical bonds between polymer chains having mechanical properties similar to chemical gels. Weak physical gels have reversible links between chains and the

associations are temporarily, which means that they have limited lifetimes, breaking and changing continuously.

Chemical crosslinking requires a linear or branched polymer with small molecular weight, difunctional or multifunctional crosslinking agent. This agent usually links two polymer chains through its functional groups. In most cases, this reaction is performed in solution for biomedical applications. The solvent mostly used for these reactions is water, but some organic solvent, such as ethanol, benzene and chloroform are also used. The second method is copolymerization reaction, which is used to chemically synthesize a copolymer and the initiators used in this reaction are radical and anionic initiators. Four steps to crosslink are initiation, propagation, crosslinking, and termination. The third method involves a combination of monomer and linear polymeric chains that are crosslinked by interlinking agents. Moreover, some of these techniques can also be performed by high energy radiative processes (e.g., gamma rays, X-rays, electron beam radiation) to form hydrogels. For instance, poly(N-vinyl-2-pyrrolidone) (PVP) can produce hydrogel with UV radiations [94]. Recently, Sperinde et al.[95] provided a novel method, enzymatic crosslinking, to synthesize PEG-based hydrogels.

2.3 Naturally derived materials

Naturally derived hydrogel forming polymers have been widely used in biomedical applications because they have similar, often identical properties to the natural extracellular matrix. An overview of some of the most commonly used proteins and polysaccharides for tissue engineering is presented below.

2.3.1 Collagen

Collagen is one of the most widely used tissue-derived polymers and a major ECM protein existing in mammalian tissues. It has a unique helix structure. Collagen can be crosslinked through both physical and chemical ways. Physically crosslinked collagen gels are reversible and have limited mechanical properties. Chemically formed gels provided better physical properties, but still have some weak points: they have poor physical strength, and are potentially immunogenic and expensive [96]. Because of its superior biocompatibility, collagen has been used as a 3D tissue scaffold [97] or artificial skin [98]. Recently research focuses on the optimization of collagen-based biomaterials for pharmaceutical applications by enhancing their mechanical properties, biodegradability and delivery characteristics.

2.3.2 Hyaluronic acid (HA)

Hyaluronic acid (HA) is a naturally occurring linear polysaccharide consisting of repeated disaccharide units. The structure of HA is composed of repeating disaccharide units α-1,4-D-*glucuronic acid* (GlcUA) and β-1,3-*acetyl-D- glucosamine* (GlcNAc)(Figure 2.1) with a molecular weight ranging from 10^3 to 10^7 Da [99]. It can be found in body fluids and tissues, such as synovial fluid, extracellular matrices, connective tissues and organs of all higher animals [100]. HA as one kind of the

glycosaminoglycans (GAGs) has been highly negatively charged due to the carboxyl groups on the HA chain that provide the molecule their negative charges. It makes the molecule extremely hydrophilic so that it can highly extend in aqueous solution and occupies extraordinary volume compared with its mass.

HA was known for its applications in cartilage, vitreous humor and ECM of skin [101]. In addition, HA has been found to bind to some kinds of plasma membrane receptors on the surface of cells in the body. Two major receptors are CD44 and the receptor for hyaluronic acid mediated motility, RHAMM [102]. All HA binding receptors contain two positively charged amino acids, Arg and Lys, that cause them to bind to the negatively charged carboxyl groups on HA. Although HA hydrogels show non-adhesion to cells, when modified with adhesive peptides, such as the adhesive fibronectin peptide fragment: Arg-Gly-Asp-Ser (RGDS), and then binding to cell receptors, HA can directly influence cell behavior.

Pure HA has a high degradation rate in vivo because of hyaluronidase. A variety of modifications and crosslinking strategies have been tried to improve the strength, toughness and durability of HA [20]. The chemical modifications of HA include two commonly used functional groups of its structure: carboxyl groups on the GlcUA subunits and hydroxyl groups. The carboxylic acid groups are often modified by esterification [103] and carbodiimide-mediated dihydrazide reactions [20, 104] to form ester linkages, whereas hydroxyl groups can be used to form ether linkages. Carbodiimide-mediated coupling of HA to primary amines has been confirmed in a variety of studies that the amide bonds could not be formed efficiently and crosslinked easily [105] till the reactive intermediate rearranges rapidly to a stable

N-acylurea adduct. But it should be noted that since the carboxyl groups of HA engaged cell surface receptors, any crosslinking or chemical modification involved the carboxyl group (including carbodiimide-mediated coupling reactions) is predictable to decrease the specific biological functions associated with HA [106].

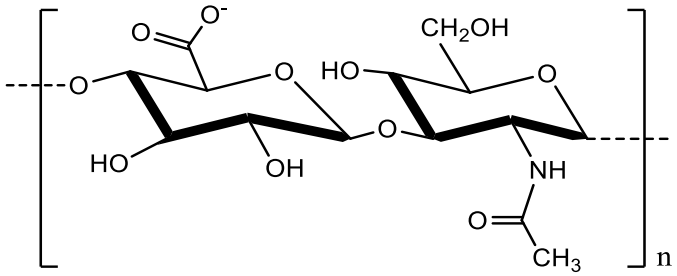

GlcUA **GlcNAc**

Figure 2.1 The chemical structure of hyaluronic acid consisting of GlcUA and GlcNAc.

2.3.3 Alginate

Alginate, also known as algin or alginic acid, is a well-known biomaterial distributed in the cell walls of brown algae. The units which make up this linear copolymer include β-D-mannuronate and α-L-glucuronate units [107]. The molecular weight ranges from 10 to 1000 kDa depending on the source and the process of its production. Alginate has a number of outstanding properties such as low toxicity, biocompatibility, relatively low cost. It can form gel simply with divalent positive ions. It has found frequent usages as microcarriers for cell encapsulation, wound dressing, immobilization matrix, dental impression and so on [108]. Although alginate has many advantages, a potential obstacle in using alginate gels in tissue engineering is the shortage of cellular interaction. In order to solve this problem, cell-interactive peptides (e.g., RGD) or growth factors can be coupled to alginate

gels to enhance cell adhesion [109]. In addition, the molecular weights of many alginate gels are above the renal threshold of the kidney [110]. A remarkable way to control the degradation of alginate has been reported recently. It includes the isolation of polyguluronate blocks with molecular mass of 6000 Da from alginate, then the derivatives crosslinking with adipic acid dihydrazide [111]. The mechanical and degradation properties of polymers could be controlled depending on the density of crosslinking[93].

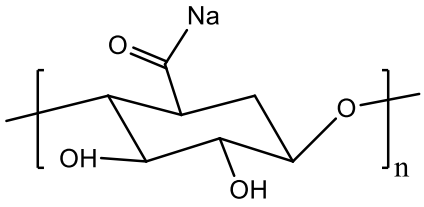

Figure 2.2 The chemical structure of sodium alginate

2.3.4 Chitosan

Chitosan is an N-deacetylated derivative of chitin which is obtained from the shells of crabs or shrimps. It has found many biomedical applications due to its biocompatibility, biochemical activity and low toxicity. It can be degraded in the presence of enzymes such as chitosanase [112]. Chitosan has good water solubility with a pH <6.2 [113], but is generally insoluble in neutral conditions and in most organic solvents due to the neutralization of the amino groups and its high crystallinity. Therefore, many approaches have been reported to improve the solubility of this polymer, such as introducing glucosamine branches [114]. Chitosan can form hydrogel ionically [115] or by chemical cross-linking with di- or

polyaldehydes [116]. The gelation rate was increased by increasing the concentration of either chitosan or aldehyde [113]. The scaffold applications of chitosan-based hydrogel in tissue engineering have also been studied. Chitosan hydrogel can be applied either itself [117] or as part of composites with synthetic polymers [118, 119], ceramics [120, 121] or natural polymer [122] aiming at different applications.

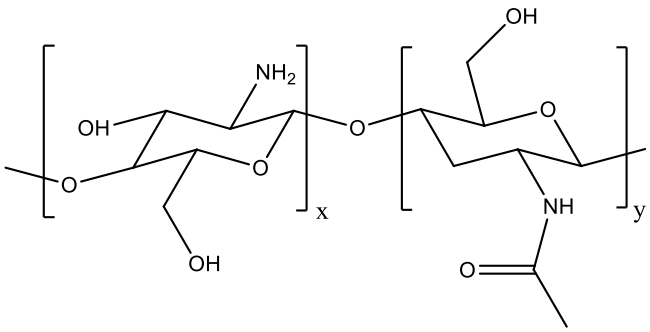

Figure 2.3 The chemical structure of chitosan

2.4 Cell adhesion

2.4.1 Cell adhesive proteins and peptides

Cells in the body do not simply “stick” together to assemble three-dimensional tissues, but rather are composed into diverse and unique patterns [123]. They also contain receptors on their surfaces, with which can bind to the underlying material through some specific proteins, such as fibrinogen, fibronectin, laminin and vitronectin [124]. Traditionally speaking, cellular adhesion on biomaterials is realized through the nonspecific adsorption of proteins to their surfaces. Researchers have found that several distinctive amino acid sequences that exist in the larger cell adhesive protein molecules also mediated adhesion, which means that direct binding of these sequences or the cell adhesive protein molecules on the biomaterials could stimulate cell adhesion and other cellular responses [125]. However, the use of proteins has a number of disadvantages for the applications of biomaterials. First of all, large proteins have to be isolated and purified. They may elicit immune responses and increase infection risks. Furthermore, these proteins can become denatured or unfolded, which could cause the receptors on the cells surface to no longer recognize them. In order to avoid proteins’ degradation, they need to be refreshed continuously. Inflammation and infection can even accelerate the degradation rate, so that long-term applications of these materials seem impossible. Due to the orientation of the protein is stochastic on a surface, it is limited if only the active site for binding is available to cells [126].

Conversely, small immobilized peptides sequences can overcome most of the problems. They are more stable, show higher stability towards sterilization and

storage conditions [127]. They can be packed with higher density on surfaces due to their lower space requirement; They can be chemically synthesized without be isolated from other organisms [125]. The peptide sequences bonded to surfaces could be displayed in a manner such that nearly all of them were active and available for binding to cell surface receptors [128]; some small peptides can even help against degradation.

2.4.2 Most commonly used cell adhesive peptides

A number of cell adhesive peptide sequences that exist in the proteins are being extensively researched. The main sequences used in the literature include RGD, REDV, YIGSR and IKVAV.

RGD was originally derived from the protein fibronectin. Since its original discovery, RGD sequences have been identified in a variety of other proteins mediating cell adhesion (e.g., vitronectin, laminin, fibrinogen, collagen) [125].

The integrin receptor α4β1 offers a target that is present on the endothelial cell but not the blood platelet. But this receptor lack of selectivity so that only can address by REDV, a tetrapeptide derived from the protein fibronectin, which has found can achieve cell-type selectivity [129].

The sequences YIGSR and IKVAV domain from laminin, has been used in the literature for nerve regeneration. YIGSR binds to the 67 kDa laminin receptor (67LR) on cell surfaces. YIGSR peptide has been found to promote adhesion and spreading of a variety of cell lines and several types of nerve cells [130-132]. IKVAV binds to a 110 kDa laminin binding protein on cell surfaces and has been found not only to

mediate neuronal attachment and growth, but also to promote the sprouting of neurites, the projections extending from neurons [133].

In our design, the cell adhesive peptide RGDS needs to be caged before it is covalently linked to thiol-modified hyaluronic acid hydrogels, and then uncaged selectively using a photomask by exposure to UV light, creating patterns on the gel which can form cell adhesive and non-adhesive areas. This design will allow the axons' directional growth from one end of the site of injury to the other site, helping the spinal cord to regenerate.

3 Hypothesis and Objectives

3.1 Project goals

Thiolated hyaluronic acid (HA-SH) has been specifically studied for drug delivery applications, but it has not been investigated as a SCI repair implant device. The aim of this study is to develop a three-dimensional cell patterning scaffold, shown in Fig. 3.1, which would possibly be designed and realized to make the broken spinal cord reconnect and fix the SCI.

3.2 Hypothesis

Thiolated HA can be chemically modified and crosslinked to form a three-dimensional hydrogel for spinal cord injury repair applications.

3.3 Objectives

1) Create a novel process to form a HA-SH hydrogel which will eventually be incorporated into a biomimetic device for treatment of spinal cord injuries.
2) Synthesize hydrogels with varying concentrations of HA-SH and different amounts of thiol groups are examined the differences among the gels.
3) Test the chemical, physical and mechanical properties of the hydrogels with varying thiol groups.
4) Study the effect of the crosslinking on the hydrogel biodegradability.

The literature review has provided with current thoughts on central nervous system regeneration, why we choose hyaluronic acid as a scaffold material, and some background information on cell adhesion. This section has provided the major ideas and objectives that are involved in the work for this thesis. This will be followed by

the experiment design, results we have achieved, and a description of the future work.

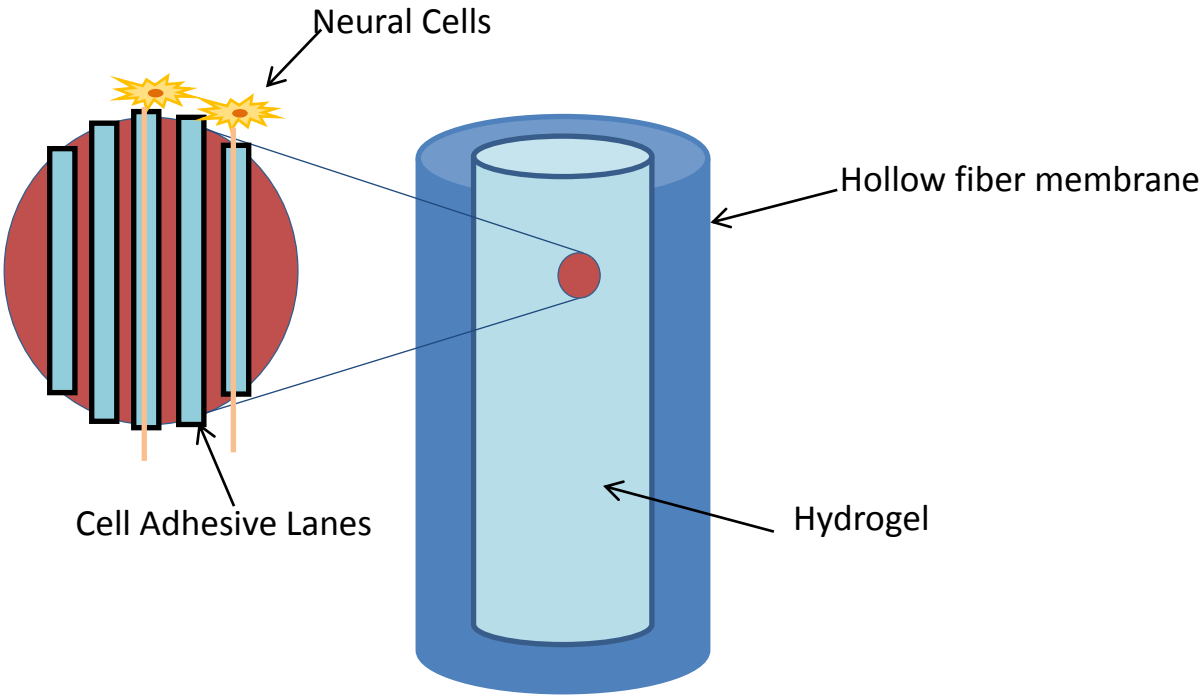

Figure 3.1 An ideal 3D micro-channel cell patterning scaffold to stimulate and direct neural cell growth in injured spinal cord.

4. Experimental Methods

4.1 Materials

Hyaluronic acid sodium salt (HA) from *Streptococcus equi* was obtained from Sigma-Aldrich (Oakville, ON). Crosslinker bismaleimide-activated PEG (1,8-Bis-Maleimidodiethyleneglycol, $BM(PEG)_n$, n=2, MW=308 Da) was purchased from Pierce (Ottawa, ON). N-hydroxylsuccinimide (NHS), Dithiotheitol (DTT), and Ethylenediaminetetraacetic acid (EDTA) were purchased from Thermo Scientific (Burlington, ON). 1-(3-dimethylaminopropyl)-3-ethyl- carbodiimide (EDC) was from VWR (Mississauga, ON). Dulbecco's phosphate buffered saline (DPBS) was from Invitrogen (Burlington, ON). All other chemicals were obtained from Sigma-Aldrich and used for the experiments as received unless indicated otherwise.

4.2 Synthesis of thiolated-hyaluronic acid (HA-SH)

The covalent bond between sodium hyaluronic acid and L-cysteine ethyl ester hydrochloride was formed via the formation of amide bonds between activated carboxyl group of hyaluronate and primary amino group of L-cysteine. HA-SH was prepared as previously described by others with minor modifications (see Figure 4.1 to 4.3 for more details of the chemistry) [20].

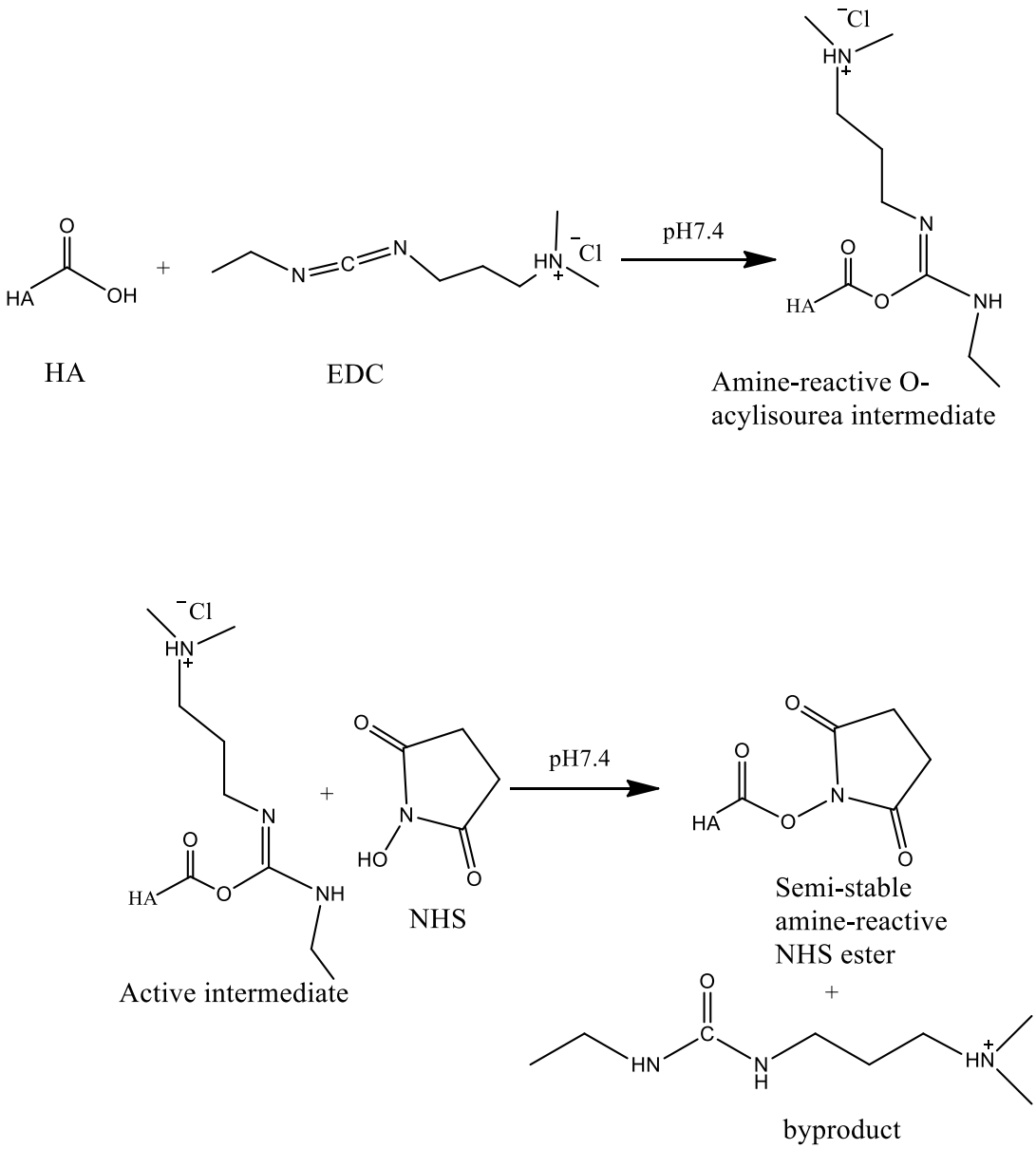

Figure 4.1 EDC/NHS coupling reaction to create amine-reactive intermediates that can improve the coupling yield.

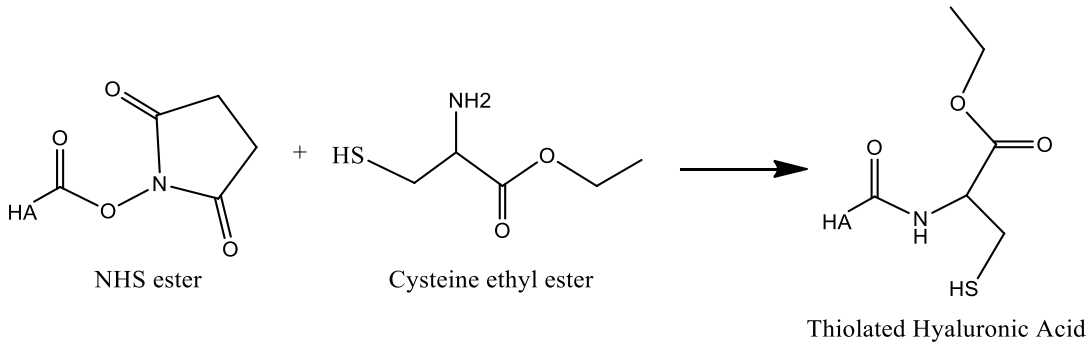

Figure 4.2 L-Cysteine ethyl ester is an amine-containing compound which can react with NHS ester

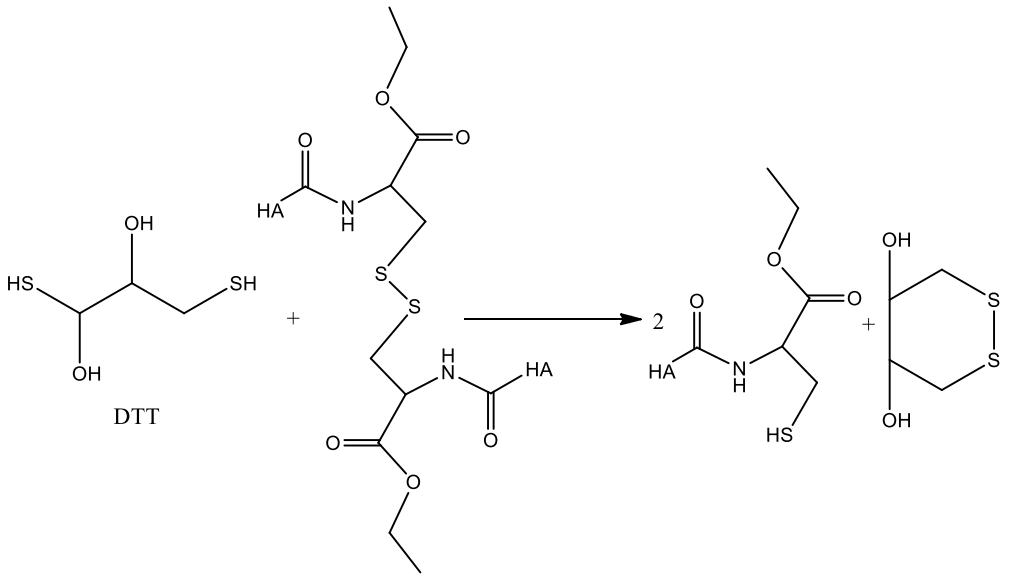

Figure 4.3 DTT added to cleave the disulfide

In a typical reaction, 0.100g HA was added into 25ml PBS (pH 7.4) under constant stirring overnight at ambient temperature to obtain a 0.4% (w/v) polymer solution. Subsequently, 431.33mg of EDC (90mM) and 258.95mg of NHS (90mM) were added to the HA solution. The reaction mixture was then stirred for 30 min at room temperature to activate the carboxyl groups on HA. To the activated HA reaction mixture, 278.51mg L-Cysteine ethyl ester hydrochloride was added and the reaction was allowed to proceed overnight at room temperature. Finally, 385.60mg of DTT (300mM) in solid form was then added to the reaction mixture to cleave the disulfide in the solution for 2 hours with stirring. The resulting reaction mixture was transferred to 6,000-8,000 MWCO FisherBrand regenerated cellulose dialysis tubing (Burlington, ON) and dialyzed twice against 1% NaCl for 24 hours to remove unreacted L-cysteine ethyl ester hydrochloride, EDC and NHS coupling agents. The samples were then purified against deionized distilled water (ddH_2O) twice. All the dialysate used here was bubbled by N_2 for 2h to remove the oxygen from the solution, added 1mM EDTA and adjusted the pH to 3 through 1mM HCl to avoid oxidation [134-136]. Finally, the samples were dialyzed against ddH_2O once to raise the pH of the mixture to neutral. The exhaustively dialyzed samples were frozen and lyophilized (Lyophilizer: Labconco Freezone 6, Kansas City, MO) to dry at -80°C, 10Pa for 2 days, and then stored at -20 °C for further use.

4.3 Determination of thiol groups

4.3.1 Fourier transform infrared (FT-IR) spectroscopy of HA-SH

The Fourier transform infrared spectrum was utilized to determine the structures of the molecules with the molecules' characteristic absorption of infrared radiation.

The HA and HA-SH lyophilized samples' FT-IR spectra were recorded to characterize the sulfhydryl group in the products, indicating the covalent attachment of L-cysteine ethyl ester hydrochloride to HA can be achieved through the reaction. An attenuated total reflectance (ATR) FT-IR spectrometer (Agilent, Mississauga, ON) was used to collect 32 scans in the 600-4,000 cm^{-1} range with a resolution of 2 cm^{-1}.

4.3.2 Ellman's test

The thiol groups immobilized on the samples were determined spectrophotometrically using Ellman's reagent which is on the basis of UV absorption of free sulfhydryl group as proposed by Riddles [137]. To carry out the test, Reaction Buffer was prepared by dissolved 1mM EDTA into 0.1M sodium phosphate buffer at pH 8.0. Ellman's Reagent Solution was prepared by dissolving 4mg Ellman's Reagent (DTNB) in 1ml of Reaction Buffer. For each sample to be tested, a tube was prepared which containing 50µl of Ellman's Reagent Solution and 2.5ml of Reaction Buffer. 5mg lyophilized HA-SH was dissolved in 10ml of reaction buffer to form a final concentration of 0.5mg/ml and split into three aliquots. Then 250µl of each sample was added to the tubes separately, mixed well, incubated at room temperature, and gassed with nitrogen for 15 minutes. The samples' absorbance at 412nm was measured with UV/VIS spectrometer (Perkin-Elmer Lambda 25, Waltham, MA).

The quantity of the free thiol groups was calculated based on a standard curve obtained by solutions with L-cysteine ethyl ester hydrochloride of known concentrations (0.0Mm-1.5mM) measured in the same way.

4.3.3 Stability of thiol groups in the lyophilized product

Lyophilized HA-SH conjugates were stored in a freezer at -20°C. At pre-determined time points (3 days), 1.5mg of each assayed sample was taken out and dissolved in 3ml reaction buffer at a final concentration of 0.5mg/ml. Aliquots of 200µl were pipetted into a vial and 50µl of 1M HCl were dripped in order to stop the further reaction[20], such as oxidation and disulfide bonds formation. The content of remaining thiol groups was determined via Ellman's reagent.

4.4 Differential scanning calorimetry (DSC) analysis

DSC characterizations were recorded by DSC Q1000 (TA Instrument, New Castle, DE), using TA Instrument Explorer software. Approximately 3-5 mg samples were added into aluminum pan at room ambient. After that, the pan with HA and the pan with HA-SH conjugate were sealed separately. Anhydrous nitrogen was used as a purge gas (purge: 20ml/min). The instrument was calibrated with pure indium (purity 99.999%, melt point 156.6°C, heat of fusion 28.45 J/g). Equilibrate at 25°C and ramp 10°C /min to 275°C.

4.5 Cross-linking of hydrogel

Each assayed sample was prepared by dissolving lyophilized HA-SH product in PBS with 5mM EDTA in 24-well plates, in a final concentration of 15mg/ml, typically 1-2ml solution contained in each well. After the samples were dissolved, ice bath was used to control the reaction rate during the crosslinking process. The amount of maleimide crosslinker $BM(PEG)_2$ added was based on the molar ratio of thiol groups in HA to carbon-carbon double bonds in $BM(PEG)_2$. Theoretically for 100% crosslinking, two moles of thiol group in HA indicates that one mole of crosslinker

should be added. However, in practical applications, two-fold molar excess $BM(PEG)_2$ added in the solution is acceptable in the reaction. Crosslinker Stock Solution was first prepared by dissolving 6.2mg $BM(PEG)_2$ in 100µl DMSO. Afterwards, the reaction mixtures were kept at RT for a few hours before incubating in PBS at 37°C.

4.6 Rheological analysis

The viscoelastic mechanical properties of the HA-SH hydrogels were characterized by a Brookfield R/S Plus rheometer (Middleboro, MA) fitted with a 50mm conical spindle with 2° cone angle. For rheology analysis, 1.5ml of each hydrogel sample was prepared by dissolving in PBS (pH 7.4) at the concentration of 30mg/ml. After the thermostat warmed the metal plate onto which the hydrogel will place to 37°C, the crosslinker was quickly added in the sample and mixed well. The mixture was then quickly placed on a metal plate which was below the spindle of the rheometer. The spindle was then immediately lowered to a gap size of 4µm so it could completely contact with the solution. Indicated viscosity was determined with time at a constant shear rate $5s^{-1}$. The *Rheo3000 v1.2* software was used to monitor the rheological properties in terms of viscosity (Pa·s) and time to gelation (s). The time at which the maximum viscosity was reached was considered to be the material's time to gelation.

4.7 Water content of hydrogel

The water-absorbing capacity of the hydrogel was determined by gravimetric method. HA hydrogels were synthesized according to the method mentioned in Section 4.2 and cut into defined shapes, dried in a vacuum oven and weight. The

weight of each hydrogel was recorded as the dry weight at t=0 (M_0). The hydrogels were then immersed in 1ml PBS buffer and incubated at 37°C for 24hours. The hydrogels were removed from the buffer and excess buffer was gently blotted away on the surface by kimwipe, to measure the mass (M_a). For all the hydrogels had been tested, a relatively constant mass was achieved after 24hrs of hydration in PBS. From these data, water content of the hydrogels was calculated as following:

$$\%\text{water} = (M_a - M_0)/M_a \times 100$$

4.8 In vitro enzymatic degradation assay

In order to determine the stability of the HA-SH hydrogel, samples of HA-SH hydrogels were synthesized in pre-weight vials, cut into defined shapes and dehydrated in the vacuum oven. Afterwards, the hydrogels were fully swollen in DPBS at 37°C for 24 hours, and the initial mass was recorded as M_i. *In vitro* degradation of HA was performed by incubating the hydrogels with 200 U/ml hyaluronidase (HAase) in DPBS at 37°C. Supernatant was removed at each predetermined time points, hydrogels were weighed (M_t), and the percentage of equilibrium mass was calculated as the following formation:

$$M_t/M_i \times 100$$

Fresh DPBS containing 200 U/ml HAase were then replaced in each sample at each time point. Hydrogels incubated in DPBS at 37°C with no enzyme were used as a control group to make a comparison of degradation analysis.

4.9 Statistics

All statistical analyses were performed using Student's t-test (two-tailed), $p<0.05$ was set as the criterion for statistical significance. The data are represented as the mean±standard deviations.

5. Results and Discussion

5.1 Synthesis of Thiolated HA

The well-established carbodiimide coupling method has been broadly used for activating the carboxyl group on polysaccharides. In our study, thiolated hyaluronic acid was successfully synthesized through forming amide bonds between carboxylic acid groups on HA chain and amine groups of cysteine ethyl ester (Scheme 5.1). Images for the HA-SH conjugate lyophilized products are shown in Figure 5.1.

EDC reacts with the carboxyl groups of HA first and forms an amine-reactive *O*-acylisourea intermediate [138]. However, the intermediate is unstable in aqueous solutions, and the hydrolysis may cause the yield of thiol moieties decreasing. *N*-hydroxysuccinimide (NHS) or its water-soluble analog (Sulfo-NHS) is often added in EDC coupling reaction to create amine-reactive intermediates that can improve the coupling yield. The hydrolysis of NHS esters' reaction rate is much slower than that of these active esters with primary amino groups at pH 6.0-7.5. Mediated by carbodiimide and N-hydroxysuccinimide, thiol groups on L-cysteine ethyl ester were introduced into HA to get the aimed product (HA-SH). The lyophilized samples were white, appeared to be of fibrous structure, almost like cotton.

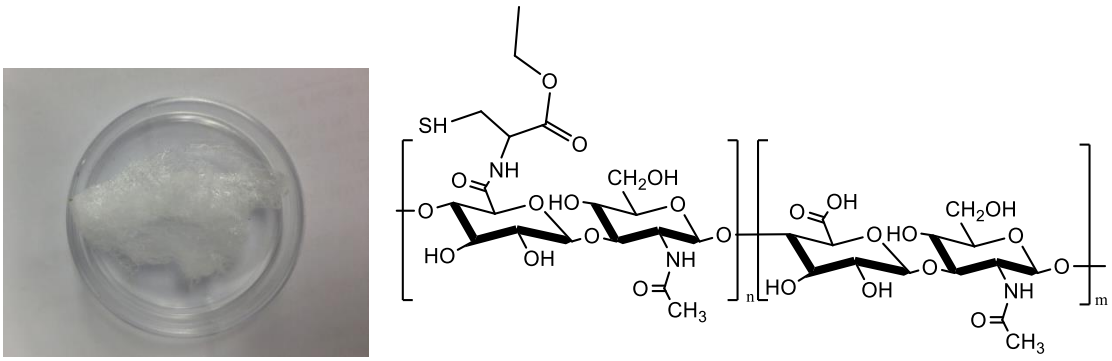

Figure 5.1 Lyophilized HA-SH. The sample is a white, fibrous structure.

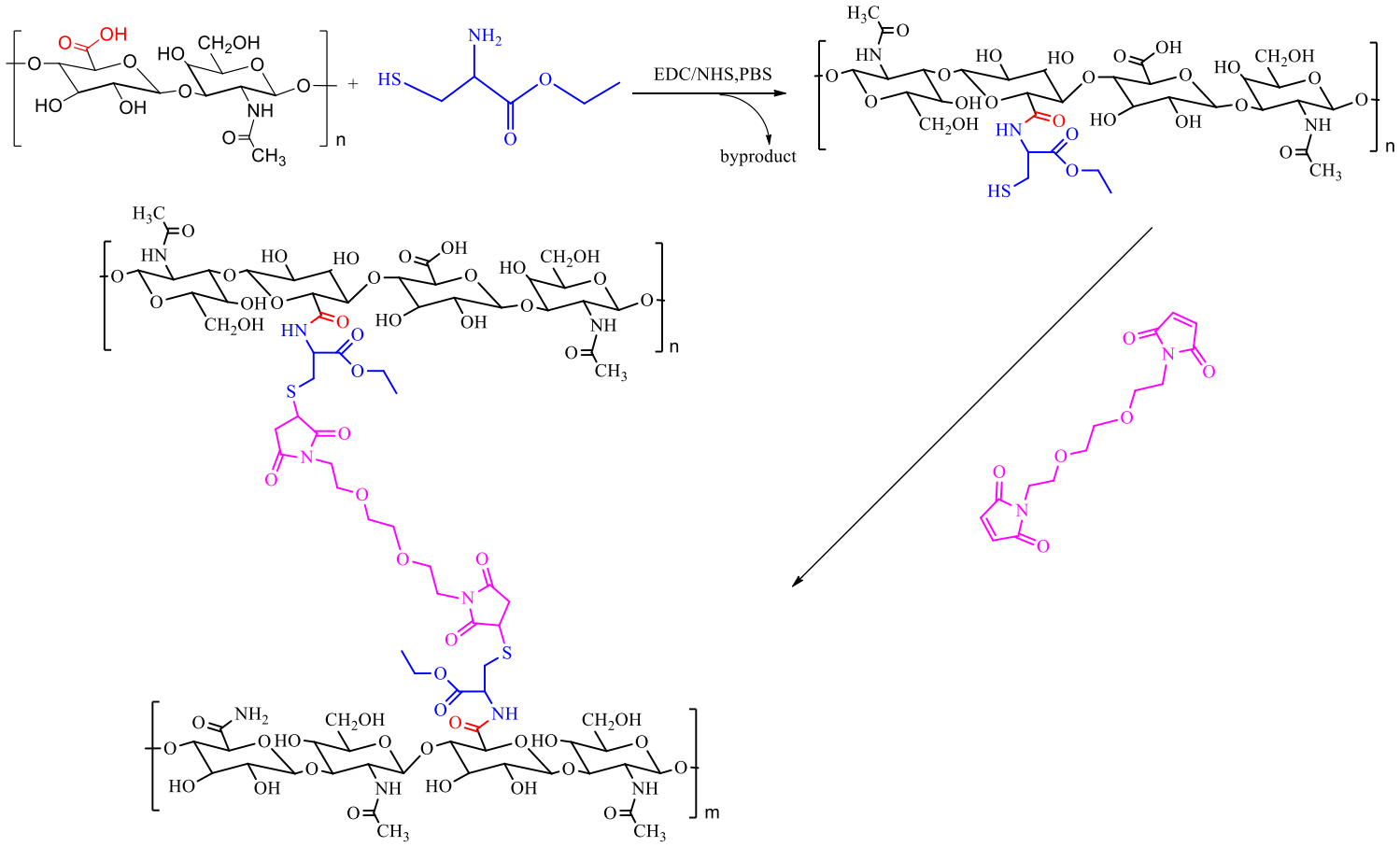

Scheme 5.1 Synthetic scheme of the thioled HA and HA-SH hydrogel preparation

5.2 FT-IR characterization

The presence of thiol functional groups on HA was confirmed by FT-IR spectroscopy. Figure 5.2 shows the FT-IR spectra of HA and HA-SH. Both of them have saccharide characteristic peak at 1300-1000 cm^{-1}(C-O-C), amide bonds peak at 1650-1550 cm^{-1} and a board band of O-H stretch (3500-3200cm^{-1}). Compared with the original hyaluronic acid, there are no significant differences between these two spectra, apart from a new small peak at 2400-2600 cm^{-1}. The peak at 2557 cm^{-1} can be attributed to the coupling of cysteine ethyl ester on the HA polymer chain, which is the characteristic transmittance peak of –SH stretching vibration area [139].

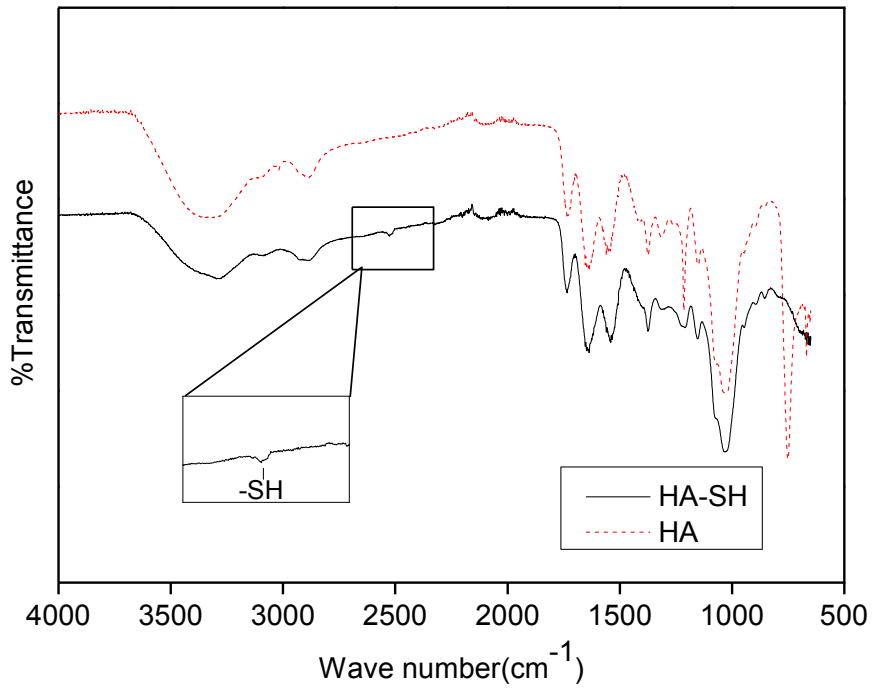

Figure 5.2 FTIR spectra of hyaluronic acid and HA-SH.

5.3 Experiment design

5.3.1 Conditions design

The method to synthesize thiolated hyaluronic acid involves forming amide bonds between the carboxyl groups on HA and amine groups on L-cysteine ethyl ester. The reaction of HA with EDC and NHS activates the carboxylic acid groups on HA, which is the site for the incorporation of an amine-containing compound. Table 5.1 shows the influence of several reaction parameters under different conditions on thiol replacement. However, thiol (-SH) is an active group, which could create a disulfide bond in aqueous solution [140]. For the L-cysteine ethyl ester, five-fold excess of DTT was added as reducing agent in the reaction mixture to reduce disulfide bonds. A Control was prepared in a similar way as hyaluronan-cysteine conjugates but omitting EDC/NHS during the coupling reaction for comparing with other samples and testing the accuracy of the procedure. The following experiments are based on this design.

	Hyaluronic acid	EDC/NHS	L-Cysteine ethyl ester	DTT
HA-SH 1X	20mM	30mM	20mM	100mM
HA-SH 2X	20mM	60mM	40mM	200mM
HA-SH 3X	20mM	90mM	60mM	300mM
HA-SH 4X	20mM	120mM	80mM	400mM
HA-SH 5X	20mM	150mM	100mM	500mM
HA-SH 6X	20mM	180mM	120mM	600mM
Control	20mM	0	60mM	300mM

Table 5.1 Experiment design to test the effect of different conditions on thiol substitution of the products: (a) The ratio of HA to EDC/NHS; (b) the ratio of HA to L-cysteine ethyl ester.

As the Fig 5.4 shows, the thiol content is an important parameter to control for gel formation, and it strongly depends on the molar ratio of HA: EDC/NHS: thiol group. By maintaining all other conditions constant, increasing the concentration of EDC/NHS in the reaction mixtures, the quantity of activated carboxyl groups is hypothesized to increase as well. In other words, it can also be described as an increase in the amount of NHS-esters [141]. Consequently, more L-cysteine ethyl ester can be incorporated into HA thus increasing the free thiol groups on HA. In addition, increasing the concentration of L-cysteine ethyl ester would also increase the amount of thiol-containing molecules in the reaction mixture which will react with NHS-ester and thus increase the quantity of thiol groups. The experiment is designed to increase the concentration of EDC, NHS, L-cysteine ethyl ester and DTT altogether for each sample to verify the hypothesis.

There are also some variations in the suggested pH of the EDC/NHS coupling reaction. For example, Kafedjiiski *et al*. performed the reaction at pH 5.5 whereas an instruction about protein-protein coupling using EDC/NHS which is published by Pierce claimed that the activation reaction proceeds most efficiently at pH between 4.5 and 7.2. EDC reactions are often performed at pH 4.7-6.0 and NHS-ester reactions are usually performed in phosphate-buffered saline (PBS). According to these previous publications [20, 142, 143], the carbodiimide-mediated coupling of HA to primary amines did not lead efficiently to the formation of amide bonds. Meanwhile, when NHS is added to the reaction, it can cause the formation of a non-rearrangable intermediate product and thus improve the coupling yields.

Therefore, we chose to investigate the effect of HA: EDC/NHS molar ratio and HA: L-cysteine ethyl ester molar ratio on the final thiol content of the prepared HA-SH samples. The goal of this design was to create a screening design for those relative factors and to gauge the factors' effect. All the reactions are performed in PBS buffer, because it can provide relatively stable conditions and suitable pH range for the reactions.

5.3.2 Solubility of lyophilized HA-SH samples

The solubility of the thiolated HA was measured by dissolving the samples in PBS buffer. Six kinds of HA-SH denoted from HA-SH 1X to HA-SH 6X were generated with various concentrations of EDC, NHS, DTT, and L-Cysteine ethyl ester (Table 5.1). The products showed insoluble property when the ratio HA: EDC/NHS: L-cysteine ethyl ester rose. The mean dissolution times of HA-SH 4X and HA-SH 5X were more than 2 hours in buffer for the concentration of 15mg/ml. This was unexpected because none of the literature reported this issue for derivatized HA. The results obtained by Shu *et al.*, which used one kind of thiolated HA derivative, suggested that the HA-SH should dissolve very well (30mg/ml used in the experiments) [31]. However if the coupling rate is too high, the material may already be crosslinked due to oxidation, resulting in insolubility. In order to avoid oxidation, some samples were prepared under nitrogen, but it did not improve the solubility. In contrast, the samples synthesized under inert atmosphere were hard to dissolve but showed higher concentration of free thiol group. The phenomenon was noted during the experiment but not gauged for insolubility. Because of the carboxyl groups on the HA chain provide the molecule its negative charge which will make the molecule extremely hydrophilic, the insolubility phenomenon may be explained by the thiol group of HA-SH substituting the carboxyl group in HA to the effect that less hydrogen bonds can form in the sample and which makes it hydrophobic in relation to HA. However, the HA-SH 6X sample turned cloudy during the process, and it could not form hydrogel when crosslinker was added. For this reason, all the samples of HA-SH 6X were discarded and the experiments of HA: EDC/NHS molar ratios more than 6 were put on hold. It was hypothesized that too much EDC added

in the system would interfere with the system and react with polymer which contain carboxyl group, and induced precipitation of the material [144]. In the end, 4X to 6X samples were discarded.

5.3 Ellman's test

Measuring the side thiol content of the samples was meant to determine the successfulness of the modification. Ellman's test, as described above, was used to calculate the amount of free thiol groups in the samples. A standard curve was obtained from the solutions of a known cysteine concentration (Figure 5.3). The absorbance of the samples was compared with the curve to calculate the concentration of free thiol groups in HA-SH.

As shown in Figure 5.4 the free sulfhydryl groups on the side chain of the samples were determined by measuring absorbance. The absorbance was measured in triplicates for each sample. HA-SH 1X, HA-SH 2X showed 163.4±28.8μmol/g and 400.0±56.3μmol/g thiol groups respectively, the sample HA-SH 3X exhibited a maximum of 488.4±95.9μmol/g immobilized free thiol groups, meaning that HA: EDC/NHS ratio increase leads the growth of sulfhydryl groups ($p<0.05$). The controls omitting EDC/NHS during the coupling reaction resulted in a negligible amount of thiol groups: 19.1±14.9μmol/g.

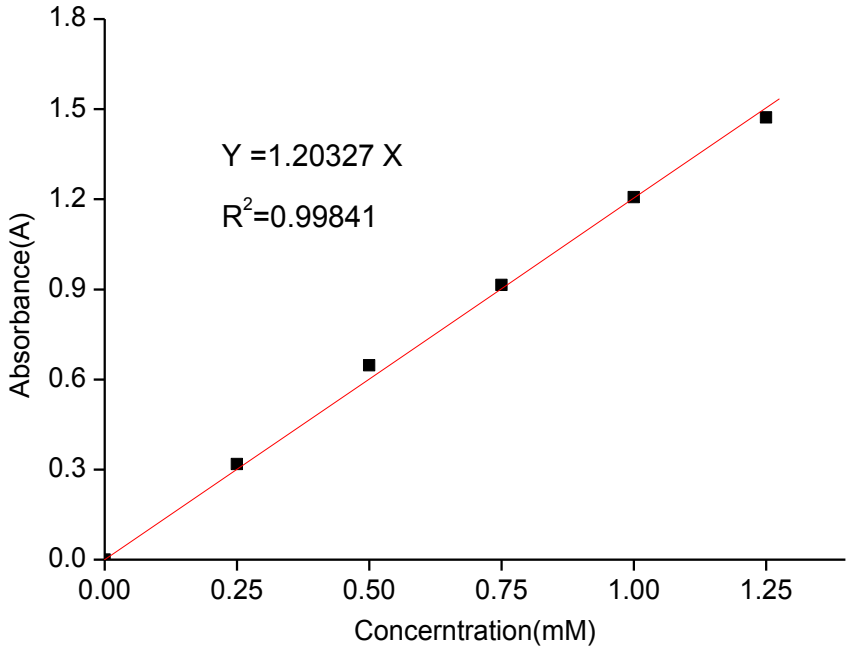

Figure 5.3 Standard curve of absorbance at 412nm for solution of varying amount of L-cysteine ethyl ester hydrochloride.

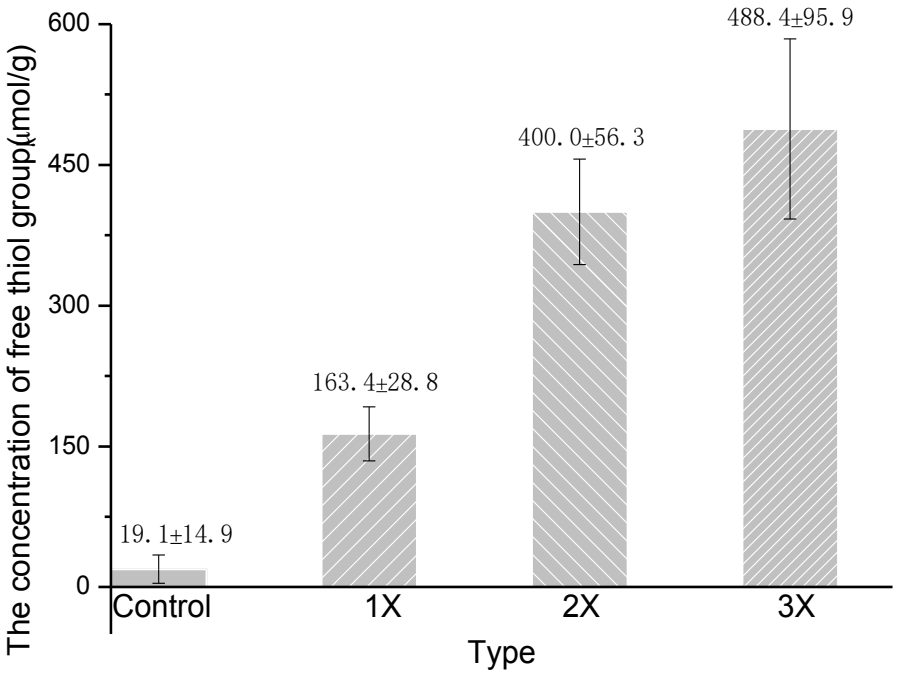

Figure 5.4 Ellman's test results of lyophilized HA-SH. Error bars represent one standard deviation. Columns represent mean±S.D., n=6 (1X, 2X and 3X, $p<0.05$ versus the control group).

5.4 Oxidation of thiol groups

To characterize the storage period of the product, the decrease of thiol groups was quantified as a function of time. The oxidation experiments were conducted under a standard storage condition at −20 °C in a sealed container, and the thiol groups were measured through Ellman's assay. The results of this study are shown in Figure 5.5. A relatively rapid formation of the disulfide bonds was observed in the first 15days of storage and was followed by a comparatively lower oxidation process in the next few days. HA-SH 3X showed outstanding stability among the three samples (1X, 2X and 3X) with 38% thiol group loss after 15days. At the end of the process, at least 40–50% of thiol groups remained available to react.

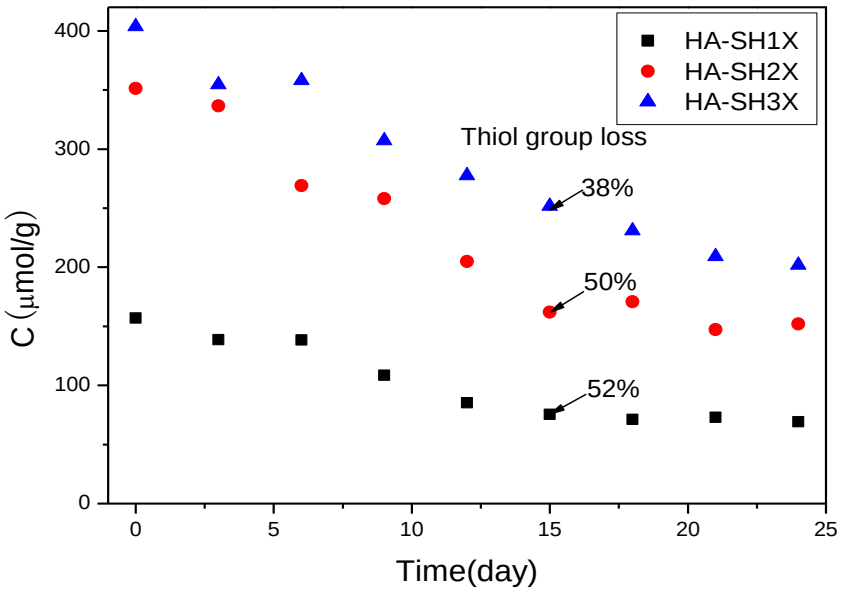

Figure 5.5 Decrease of the thiol groups (Under storage -20°C dry sample).

5.5 DSC analysis

The thermal behavior of the HA and thiolated HA was investigated by DSC in nitrogen atmosphere. The themograms are shown in Figure 5.6. Under nitrogen atmosphere, HA shows an exothermic peak at 222°C. Such a process was attributed to be the decomposition of the polymer, resulting into a carbonized residue. The data published previously demonstrated HA thermal resistance at least up to 150°C [145, 146]. Moreover, Villetti *et al.* reported that a degradation of sodium hyaluronate could be caused by increasing the temperatures above 200°C in a nitrogen atmosphere. The exothermal peak occurring in the temperature range of 200-250°C is related to the conformation change of polysaccharide—the cleavage of β-(1-4) glycosidic bond in the backbone [147]. Thermal degradation processes of thiolated derivate showed similar behavior as hyaluronic acid, and had an exothermic peak at 198°C. The comparison presented in Fig. 5.6 shows that the thermal behavior of HA and HA-SH differs mainly in intensity of released heat during decomposition in the first step and in the intensity of peak maxima. Moreover, the intensity ratio of peak maxima differed significantly. Therefore, the modified HA caused a shift to lower decomposition onset temperatures in comparison with HA (difference of 24°C).

Thermal analysis is an important method because heat is commonly used in industrial processes, and the thermal decomposition data relates to materials' stability and the residues of its decomposition.

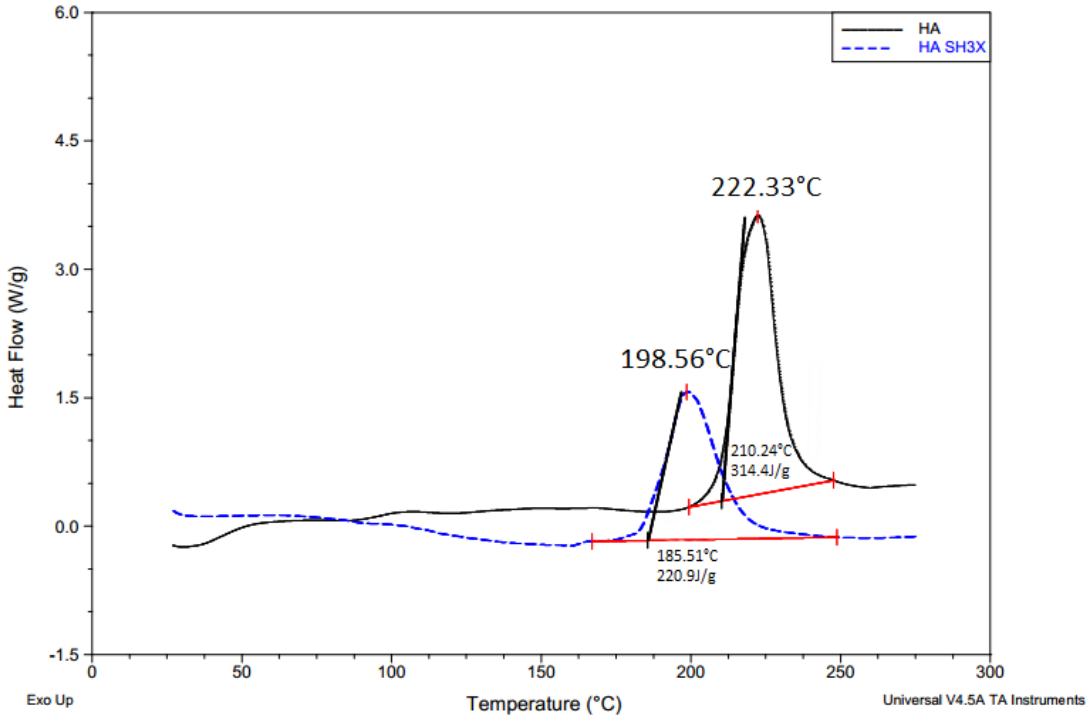

Figure 5.6 Comparison of DSC records of hyaluronic acid sodium salt and thiolated hyaluronic acid (HA-SH) in inert atmosphere, flow rate 20 mL min^{-1}, heating rate 10°C/min.

5.6 BM(PEG)$_2$ cross-linked HA-SH hydrogels

Several strategies have been created to synthesize thiolated hyaluronic acid (HA-SH) and then form hydrogels [20, 31, 148]. However, a common method to prepare hydrogel from thiol modified HA is disulfide crosslinking. Although this reaction is reversible and can form gels under mild conditions, the gel crosslink via disulfide bonds is time-consuming, unstable and the process is hard to monitor. In this thesis, HA-SH hydrogels with varying thiol concentrations were successfully synthesized by the protocol as described in Section 4.5. It leads to a following conjugation as shown in Scheme 5.1. The image of the hydrogel is shown in Figure 5.7.

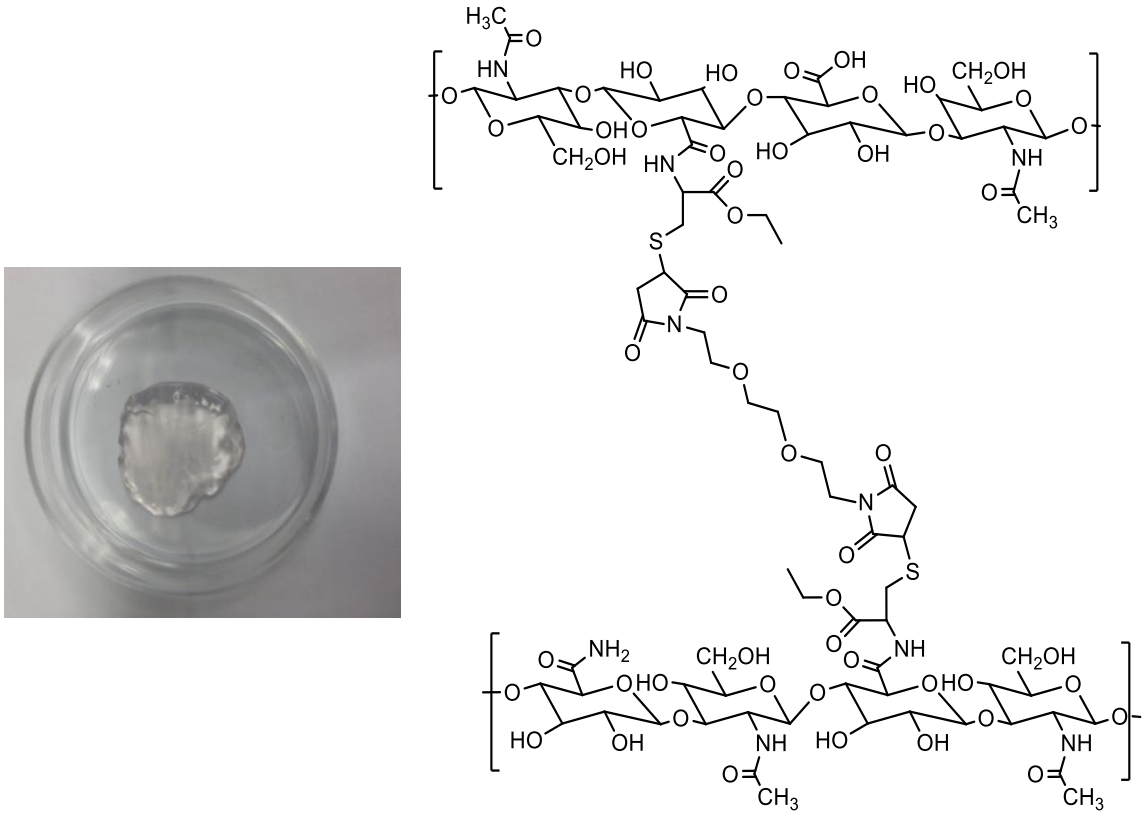

Figure 5.7 A sample of HA-SH hydrogel and its structure. The product is obtained by dissolving the lyophilized material in PBS, then adding $BM(PEG)_2$ to chemically crosslink the sulfhydryl groups on HA.

5.6.1 Attempted crosslinking

The first attempt at gelation was not successful. The main reason for the failure was due to adding 1mM HCl in the solution to avoid oxidation during dissolving. As the pH is an important parameter for gelation, the hydrogel cannot form if the HA-SH sample is out of the suitable pH range. Some reports mentioned that the pH of a solution has strong effect on hydrogel crosslinking [149, 150]. Reaction of maleimides with free sulfhydryl groups is mainly at pH 6.5-7.5 [151]. More gelation experiments were done in PBS without acid to validate this reaction condition and then gels were formed successfully. Various concentrations of HA-SH dissolved in PBS with 5mM EDTA for crosslinking were tested: 10, 15, 20, 25, 30 and 35mg/ml.

The lowest concentration of polymer that can form stable a hydrogel was 15mg/ml. Because of its insolubility, several samples which were prepared at the concentration of 35mg/ml could not dissolve completely. Therefore, the chosen concentration range to prepare the hydrogels was from 15ml/mg to 30ml/mg.

5.6.2 Transparency of hydrogels

The synthesized HA-SH hydrogel was a solid, transparent and jelly-like material. After incubation at 37°C, the hydrogel showed moisture evaporation and turned yellow. However, soaking the hydrogel in PBS would help remove the color and turn it back to clear. These color changes may have been caused by residual maleimides crosslinker which in turn dyed the gel due to $BM(PEG)_2$ having not reacted completely. After washing this phenomenon, for the remaining attempts to make HA-SH hydrogels, the excess crosslinkers were removed by washing the gels in PBS or adding a quenching solution. The hydrogels later made were all transparent ones. The quenching solutions can be found in Pierce instructions on $BM(PEG)_n$ that is prepared by concentrated (0.5-1M) cysteine, DTT, or other thiol-containing reducing agent.

5.7 Rheology

The physical characteristics, and particularly the rheological properties of a material, are important in the development of injectable hydrogels. The viscosity of the hydrogels, which is related to the stability upon implantation, was characterized by parallel-plate geometry at 37°C, which shows information about the strength of the hydrogels and the relationship between the amount of thiol groups and the gelation time. The concentration of the thiol group varies in the hyaluronic acid to modulate the gelling behavior of the material. Three types of hydrogels were evaluated: HA-SH 1X, HA-SH 2X, and HA-SH 3X. The results are shown in Figure 5.8.

Increasing the thiol content led to a reduction in time to gelation. However, the relationship was a non-linear change. The gelation time of HA-SH2X and HA-SH 3X were about 31min and 6min respectively, and both were shorter than HA-SH 1X which has the longest gelation time at about 37min. Significant differences effected between HA-SH 1X and HA-SH 3X in the gelation time. Moreover, rheological data also demonstrated a direct relationship between the concentration of sulfhydryl groups and maximum viscosity. The maximum viscosities reached for HA-SH 1X, HA-SH 2X and HA-SH 3X were 6.7 Pa·s, 46.0 Pa·s and 61.0 Pa·s, respectively. The HA-SH 1X hydrogel had the lowest relative viscosity, whereas the HA-SH 3X had the highest. As the concentration of thiol group was increased, greater viscosity of the hydrogel and a reduction in the time to gelation were observed. In other words, the strength of the hydrogel was increasing. Figure 5.8 also illustrates the apparent decline of viscosity in the curve of HA-SH 3X. This is due to the experiment being carried out in an open environment and the conical spindle having a cone angle. The curve is regulated by the cooperative and synergistic actions of many factors, such

as shear thinning, evaporation and gelation. Moreover, some pieces of HA-SH 3X hydrogel were extruded during the shearing process, causing viscosity to plummet. Rheology tests are commonly used to characterize hydrogels. The data can provide suitable injectability and allow adequate time for delivery of the material before a change in viscosity occurs [152-154].

Finally, we chose HA-SH 2X and HA-SH 3X for further experiments; HA-SH 1X was discarded because of its poor mechanical property.

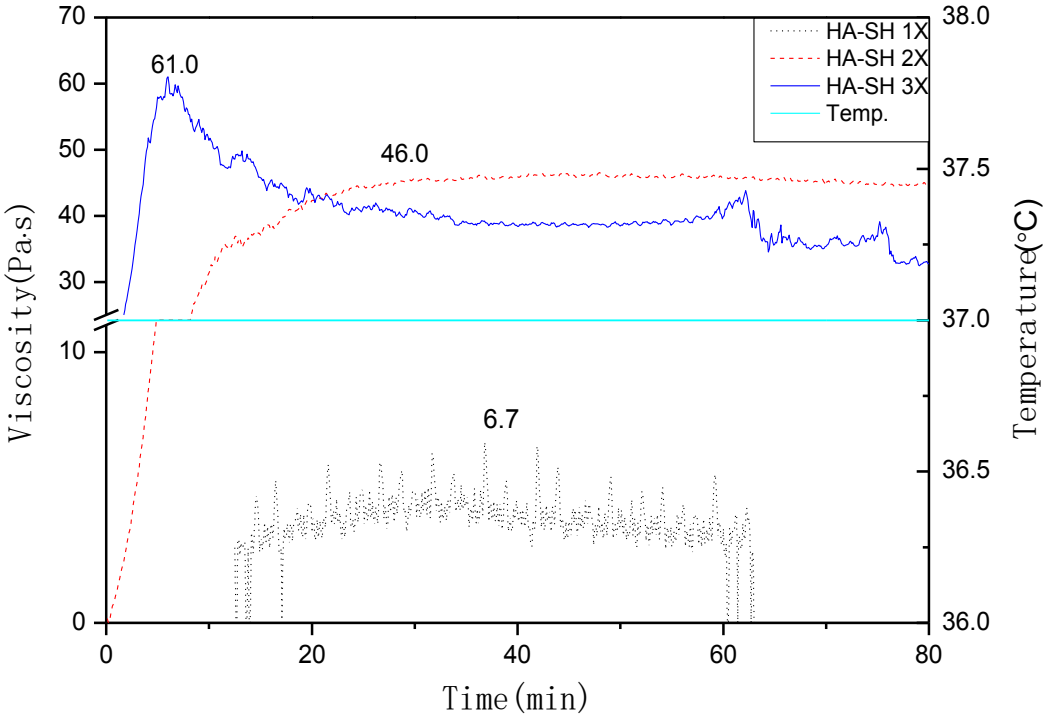

Figure 5.8 Representative viscosity–time curves for matrices with varying thiol content

5.8 Water content

The water absorbance capacity is one of the most important physical properties to characterize hydrogel. It was determined by calculating the water content of the HA-SH hydrogels which was influenced by the percentage of theoretical crosslinks and the amount of thiol group within the hydrogel. The percentage of the water content in the HA hydrogels decreased with increasing the amount of maleimide crosslinker. As shown in Fig 5.9, the water content of HA-SH 2X dropped from 95.1±0.72% to 85.2±1.92% and HA-SH 3X from 95.0±0.86% to 78.7±0.57% for 50% and 100% of theoretical maleimide crosslinker respectively. Also, the percentage of water in the hydrogels decreased when the amount of thiol group raised while keeping the amount of $BM(PEG)_2$ constant.

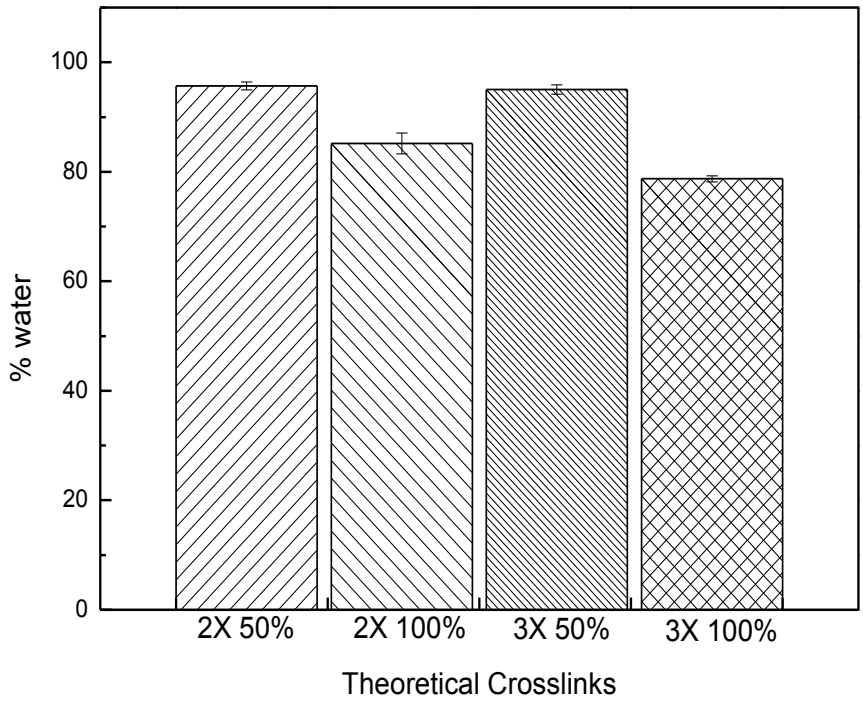

Figure 5.9 Water content of HA–SH hydrogels with different percentages of crosslinker.

5.9 Enzymatic degradation

The biodegradability of component materials is critical when designing an implantable device. The erosion process occurs either in bulk or at the polymers surface whereby release rates are related to the surface area. Researchers have been able to control the rate of drug delivery by varying each of these factors. To monitor *in vitro* degradation of HA-SH hydrogels, the samples were incubated in DPBS with 200Uml^{-1} of hyaluronidase at 37°C. The effect of hyaluronidase on the degradation of HA-SH *in vitro* is shown in Figure 5.10.

HA-SH hydrogels presented here were found to degrade in the presence of hyaluronidase (HAase) indicating that the modification of HA does not prevent biodegradation. It means that HA-SH hydrogels have potential for applications in tissue engineering. The time for complete degradation of the hydrogels in HAase depends on their thiol content and equivalents of crosslinker. The most stable hydrogels can be produced with the highest degree of crosslinking. At the same time, the samples incubated in PBS (controls) showed no significant mass loss.

Regarding HA-SH 2X hydrogels which were incubated with HAase, the gels consumed rapidly as the enzymatic reaction proceeded: over 50% of equilibrium mass loss after 72h and 26.7±15.4% remained at 96h was observed. For HA-SH 3X, the initial decrease of mass took place slower compared with HA-SH 2X, 66.79±3.1% remained at 72h and 52.9±5.7% remained after 96h was found. The maximal time for the hydrogels to degrade completely was 216h (HA-SH 2X) and 312h (HA-SH 3X) in HAase (200U/ml), which illustrated that HA-SH 3X had better stability than that of HA-SH 2X. HA hydrogels have been reported for a variety of crosslinking chemistries, such as those based on adipic dihydrazides [17] and disulfides[31]. However, for

these hydrogels, the slowest degradation rates of the adipic dihydrazides were after 4 days (96 h) for 100% degradation [17], and 36% degradation in 2 days (48h) for the disulfides [31]. The degradation rates of these hydrogels were faster than what we observed in the current study.

Furthermore, slower degradation rates for HA-SH hydrogels *in vivo* may be achieved because hyaluronidase levels in the organism are much lower than those used in this study. Though the results obtained from this experiment only monitored the thiol concentration, it verified that the HA-SH is suitable for application in tissue engineering within a certain degradation time. Thus, the hydrogel could be tailored depending on the application.

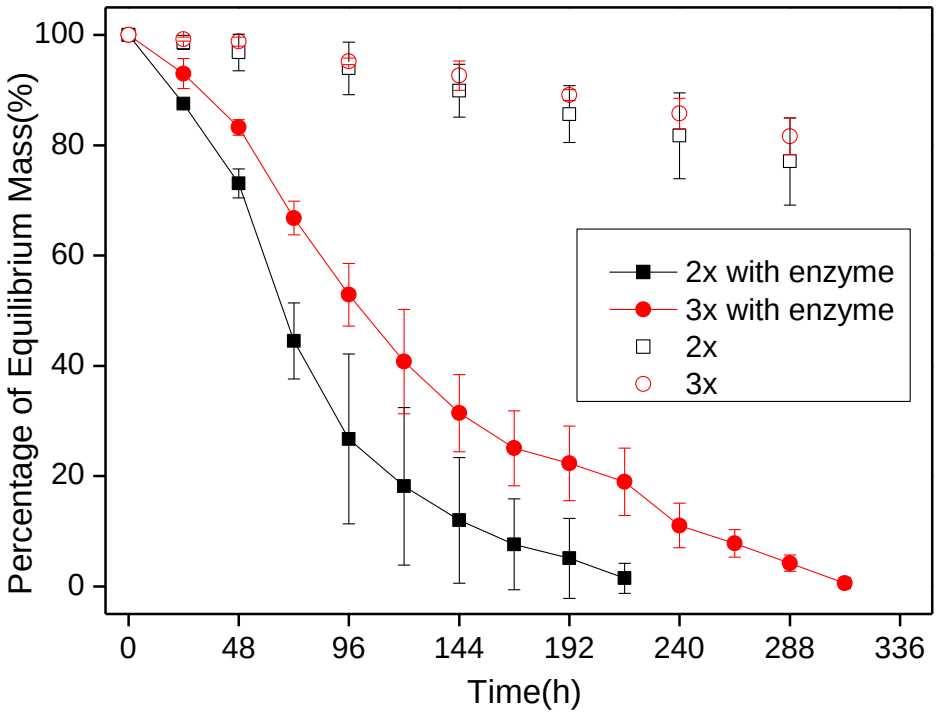

Figure 5.10 In vitro degradation of HA-SH hydrogel. Solid shapes: samples incubated in DPBS with 200 U ml-1 of hyaluronidase. Open shapes: samples incubated in DPBS (control) average percentage of equilibrium weight (standard deviation n=3).

6. Conclusions and Future work

The benefits of hyaluronic acid in tissue engineering applications have been seen in the areas of wound healing [155, 156], artificial skin [157], and soft tissue augmentation [158]. However, none of the reported in literature for HA used as an implantable device to treat SCI [159]. In this study, hyaluronic-cysteine ethyl ester conjugate was successfully synthesized and gelled through a novel method. By increasing the amount of reagents used to modify HA, the synthesized hydrogels resulted in higher thiol content and insolubility. Moreover, the hydrogels with higher thiol content showed higher viscosity. Also, increasing the degree of cross-linking in the hydrogels resulted in lower water content. Compared with unmodified HA, the significantly lowered biodegradation rate is a prerequisite for future HA-SH hydrogel to be applied in SCI treatment. Therefore, this novel thiolated polymer appears to be a very promising material for the development of implantable devices.

Our project focuses on developing a novel 3D cell patterning scaffold, which is aimed at bridging the nerve gap and could eventually be incorporated into a nerve conduit for repairing the injured spinal cord [160, 161]. In order to use the scaffold for this application, many factors need to be considered, such as the degree of crosslinking, strength of hydrogel, and biocompatibility. when developing an applicable scaffold. In this work, we characterized the chemical, physical, and mechanical properties of the biomaterial and its hydrogels.

In order to create an ideal conduit model to realize SCI therapy, the future studies that we wish to conduct can be divided into three sections with different goals:

1. To incorporate the peptide RGDS into the hydrogel.

2. To demonstrate the extent of the cell adhesion to modified hydrogel surfaces.
3. To incorporate caged RGDS in the gel, patterning in three-dimensional using a two-photon laser.

Reference

1. Inc., M.-W., *Merriam-Webster's collegiate dictionary*. 2004: Merriam-Webster.
2. Ballou, R.C., *Made to measure: New materials for the 21st century - Ball,P.* Library Journal, 1997. **122**(19): p. 73-73.
3. Ratner, B.D., et al., *Biomaterials science: an introduction to materials in medicine.* San Diego, California, 2004: p. 162-164.
4. Baldwin, A.D. and K.L. Kiick, *Polysaccharide-modified synthetic polymeric biomaterials.* Biopolymers, 2010. **94**(1): p. 128-40.
5. Peppas, N.A. and R. Langer, *NEW CHALLENGES IN BIOMATERIALS.* Science, 1994. **263**(5154): p. 1715-1720.
6. Rahimi, A. and A. Mashak, *Review on rubbers in medicine: natural, silicone and polyurethane rubbers.* Plastics, Rubber and Composites, 2013. **42**(6): p. 223-230.
7. Middleton, J.C. and A. Tipton, *Synthetic biodegradable polymers as medical devices.* MEDICAL PLASTIC AND BIOMATERIALS, 1998. **5**: p. 30-39.
8. Chandra, R. and R. Rustgi, *Biodegradable polymers.* Progress in Polymer Science, 1998. **23**(7): p. 1273-1335.
9. Fulzele, S.V., P.M. Satturwar, and A.K. Dorle, *Study of the biodegradation and in vivo biocompatibility of novel biomaterials.* European Journal of Pharmaceutical Sciences, 2003. **20**(1): p. 53-61.
10. Abdul, S. and S.S. Poddar, *A flexible technology for modified release of drugs: multi layered tablets.* J Control Release, 2004. **97**(3): p. 393-405.
11. Soppimath, K.S., et al., *Biodegradable polymeric nanoparticles as drug delivery devices.* Journal of Controlled Release, 2001. **70**(1-2): p. 1-20.
12. Ju, H.K., S.Y. Kim, and Y.M. Lee, *pH/temperature-responsive behaviors of semi-IPN and comb-type graft hydrogels composed of alginate and poly (N-isopropylacrylamide).* Polymer, 2001. **42**(16): p. 6851-6857.
13. Blaine, G., *EXPERIMENTAL OBSERVATIONS ON ABSORBABLE ALGINATE PRODUCTS IN SURGERY - GEL, FILM, GAUZE AND FOAM.* Annals of Surgery, 1947. **125**(1): p. 102-114.
14. Chandy, T. and C.P. Sharma, *CHITOSAN - AS A BIOMATERIAL.* Biomaterials Artificial Cells and Artificial Organs, 1990. **18**(1): p. 1-24.
15. Muzzarelli, R.A., C. Jeuniaux, and G.W. Gooday, *Chitin in nature and technology.* 1986.
16. Tokura, S., Y. Miura, and Y. Uraki, *BIODEGRADABLE CHITIN DERIVATIVE AS VARIOUS TYPES OF DRUG CARRIERS.* Abstracts of Papers of the American Chemical Society, 1990. **199**: p. 297-POLY.
17. Luo, Y., K.R. Kirker, and G.D. Prestwich, *Cross-linked hyaluronic acid hydrogel films: new biomaterials for drug delivery.* Journal Of Controlled Release, 2000. **69**(1): p. 169-184.
18. Zhang, J.X., A. Skardal, and G.D. Prestwich, *Engineered extracellular matrices with cleavable crosslinkers for cell expansion and easy cell recovery.* Biomaterials, 2008. **29**(34): p. 4521-4531.
19. Leach, J.B. and C.E. Schmidt, *Characterization of protein release from photocrosslinkable hyaluronic acid-polyethylene glycol hydrogel tissue engineering scaffolds.* Biomaterials, 2005. **26**(2): p. 125-135.

20. Kafedjiiski, K., et al., *Synthesis and in vitro evaluation of thiolated hyaluronic acid for mucoadhesive drug delivery.* Int J Pharm, 2007. **343**(1-2): p. 48-58.
21. Tabata, Y., et al., *SUPPRESSIVE EFFECT OF RECOMBINANT TNF-GELATIN CONJUGATE ON MURINE TUMOR-GROWTH INVIVO.* Journal of Pharmacy and Pharmacology, 1993. **45**(4): p. 303-308.
22. Kamath, K.R. and K. Park, *BIODEGRADABLE HYDROGELS IN DRUG-DELIVERY.* Advanced Drug Delivery Reviews, 1993. **11**(1-2): p. 59-84.
23. Cai, S.S., et al., *Injectable glycosaminoglycan hydrogels for controlled release of human basic fibroblast growth factor.* Biomaterials, 2005. **26**(30): p. 6054-6067.
24. Collins, M.N. and C. Birkinshaw, *Comparison of the effectiveness of four different crosslinking agents with hyaluronic acid hydrogel films for tisslue-culture applications.* Journal of Applied Polymer Science, 2007. **104**(5): p. 3183-3191.
25. Alberts, B., et al., *Molecular biology of the cell, 1994.* Garland, New York: p. 139-194.
26. Yamane, S., et al., *Feasibility of chitosan-based hyaluronic acid hybrid biomaterial for a novel scaffold in cartilage tissue engineering.* Biomaterials, 2005. **26**(6): p. 611-619.
27. Morra, M. and C. Cassineli, *Non-fouling properties of polysaccharide-coated surfaces.* Journal of Biomaterials Science-Polymer Edition, 1999. **10**(10): p. 1107-1124.
28. Park, Y.D., N. Tirelli, and J.A. Hubbell, *Photopolymerized hyaluronic acid-based hydrogels and interpenetrating networks.* Biomaterials, 2003. **24**(6): p. 893-900.
29. Jou, C.-H., et al., *Biocompatibility and antibacterial activity of chitosan and hyaluronic acid immobilized polyester fibers.* Journal of Applied Polymer Science, 2007. **104**(1): p. 220-225.
30. Nisbet, D.R., et al., *Neural tissue engineering of the CNS using hydrogels.* Journal of Biomedical Materials Research Part B-Applied Biomaterials, 2008. **87B**(1): p. 251-263.
31. Shu, X.Z., et al., *Disulfide cross-linked hyaluronan hydrogels.* Biomacromolecules, 2002. **3**(6): p. 1304-1311.
32. Venes, D., *Taber's cyclopedic medical dictionary*. 2013: FA Davis.
33. Kuthy, S., et al., *After the party's over: evaluation of a drinking and driving prevention program.* Journal of neuroscience nursing, 1995. **27**(5): p. 273-277.
34. Shults, R.A., et al., *Association between state level drinking and driving countermeasures and self reported alcohol impaired driving.* Injury Prevention, 2002. **8**(2): p. 106-110.
35. Pickett, G.E., et al., *Epidemiology of traumatic spinal cord injury in Canada.* Spine, 2006. **31**(7): p. 799-805.
36. Noonan, V.K., et al., *Incidence and Prevalence of Spinal Cord Injury in Canada: A National Perspective.* Neuroepidemiology, 2012. **38**(4): p. 219-226.
37. Munce, S.E.P., et al., *Direct costs of adult traumatic spinal cord injury in ontario.* Spinal Cord, 2013. **51**(1): p. 64-69.

38. DeVivo, M.J., *Causes and costs of spinal cord injury in the United States.* Spinal Cord, 1997. **35**(12): p. 809-813.
39. Fry, E.J., et al., *Corticospinal Tract Regeneration After Spinal Cord Injury in Receptor Protein Tyrosine Phosphatase Sigma Deficient Mice.* Glia, 2010. **58**(4): p. 423-433.
40. Filbin, M.T., *Myelin-associated inhibitors of axonal regeneration in the adult mammalian CNS.* Nature Reviews Neuroscience, 2003. **4**(9): p. 703-713.
41. Gonzenbach, R.R. and M.E. Schwab, *Disinhibition of neurite growth to repair the injured adult CNS: Focusing on Nogo.* Cellular and Molecular Life Sciences, 2008. **65**(1): p. 161-176.
42. y Cajal, S.R., *Degeneration & regeneration of the nervous system*. Vol. 1. 1928: Oxford University Press, Humphrey Milford.
43. Caroni, P. and M.E. Schwab, *Two membrane protein fractions from rat central myelin with inhibitory properties for neurite growth and fibroblast spreading.* The Journal of cell biology, 1988. **106**(4): p. 1281-1288.
44. Caroni, P. and M.E. Schwab, *Antibody against myelin associated inhibitor of neurite growth neutralizes nonpermissive substrate properties of CNS white matter.* Neuron, 1988. **1**(1): p. 85-96.
45. Schnell, L. and M.E. Schwab, *Axonal regeneration in the rat spinal cord produced by an antibody against myelin-associated neurite growth inhibitors.* 1990.
46. GrandPre, T., et al., *Identification of the Nogo inhibitor of axon regeneration as a Reticulon protein.* Nature, 2000. **403**(6768): p. 439-444.
47. Chen, M.S., et al., *Nogo-A is a myelin-associated neurite outgrowth inhibitor and an antigen for monoclonal antibody IN-1.* Nature, 2000. **403**(6768): p. 434-439.
48. Mukhopadhyay, G., et al., *A NOVEL ROLE FOR MYELIN-ASSOCIATED GLYCOPROTEIN AS AN INHIBITOR OF AXONAL REGENERATION.* Neuron, 1994. **13**(3): p. 757-767.
49. McKerracher, L., et al., *IDENTIFICATION OF MYELIN-ASSOCIATED GLYCOPROTEIN AS A MAJOR MYELIN-DERIVED INHIBITOR OF NEURITE GROWTH.* Neuron, 1994. **13**(4): p. 805-811.
50. Habib, A.A., et al., *Expression of the oligodendrocyte-myelin glycoprotein by neurons in the mouse central nervous system.* Journal of Neurochemistry, 1998. **70**(4): p. 1704-1711.
51. Hata, K., et al., *RGMa inhibition promotes axonal growth and recovery after spinal cord injury.* Journal of Cell Biology, 2006. **173**(1): p. 47-58.
52. Benson, M.D., et al., *Ephrin-B3 is a myelin-based inhibitor of neurite outgrowth.* Proceedings of the National Academy of Sciences of the United States of America, 2005. **102**(30): p. 10694-10699.
53. Schnell, L. and M.E. Schwab, *AXONAL REGENERATION IN THE RAT SPINAL-CORD PRODUCED BY AN ANTIBODY AGAINST MYELIN-ASSOCIATED NEURITE GROWTH-INHIBITORS.* Nature, 1990. **343**(6255): p. 269-272.
54. Bregman, B.S., et al., *RECOVERY FROM SPINAL-CORD INJURY MEDIATED BY ANTIBODIES TO NEURITE GROWTH-INHIBITORS.* Nature, 1995. **378**(6556): p. 498-501.

55. Becker, T., et al., *Tenascin-R inhibits regrowth of optic fibers in vitro and persists in the optic nerve of mice after injury.* Glia, 2000. **29**(4): p. 330-346.
56. McKeon, R.J., et al., *REDUCTION OF NEURITE OUTGROWTH IN A MODEL OF GLIAL SCARRING FOLLOWING CNS INJURY IS CORRELATED WITH THE EXPRESSION OF INHIBITORY MOLECULES ON REACTIVE ASTROCYTES.* Journal of Neuroscience, 1991. **11**(11): p. 3398-3411.
57. Jones, L.L., R.U. Margolis, and M.H. Tuszynski, *The chondroitin sulfate proteoglycans neurocan, brevican, phosphacan, and versican are differentially regulated following spinal cord injury.* Experimental Neurology, 2003. **182**(2): p. 399-411.
58. Braunewell, K.H., et al., *FUNCTIONAL INVOLVEMENT OF SCIATIC NERVE-DERIVED VERSICAN AND DECORIN-LIKE MOLECULES AND OTHER CHONDROITIN SULFATE PROTEOGLYCANS IN ECM-MEDIATED CELL-ADHESION AND NEURITE OUTGROWTH.* European Journal of Neuroscience, 1995. **7**(4): p. 805-814.
59. Yamada, H., et al., *The brain chondroitin sulfate proteoglycan brevican associates with astrocytes ensheathing cerebellar glomeruli and inhibits neurite outgrowth from granule neurons.* Journal of Neuroscience, 1997. **17**(20): p. 7784-7795.
60. Ughrin, Y.M., Z.J. Chen, and J.M. Levine, *Multiple regions of the NG2 proteoglycan inhibit neurite growth and induce growth cone collapse.* Journal of Neuroscience, 2003. **23**(1): p. 175-186.
61. Tester, N.J. and D.R. Howland, *Chondroitinase ABC improves basic and skilled locomotion in spinal cord injured cats.* Experimental Neurology, 2008. **209**(2): p. 483-496.
62. Moon, L.D.F., et al., *Regeneration of CNS axons back to their target following treatment of adult rat brain with chondroitinase ABC.* Nature Neuroscience, 2001. **4**(5): p. 465-466.
63. Dorland, W.A.N., *Dorland's Medical dictionary*. 1980: Saunders Press.
64. Cohen, S., R. Levi-Montalcini, and V. Hamburger, *A nerve growth-stimulating factor isolated from sarcom as 37 and 180.* Proceedings of the National Academy of Sciences of the United States of America, 1954. **40**(10): p. 1014.
65. Durany, N. and J. Thome, *Neurotrophic factors and the pathophysiology of schizophrenic psychoses.* European psychiatry, 2004. **19**(6): p. 326-337.
66. Raedler, T.J., M.B. Knable, and D.R. Weinberger, *Schizophrenia as a developmental disorder of the cerebral cortex.* Current Opinion in Neurobiology, 1998. **8**(1): p. 157-161.
67. Lu, P. and M.H. Tuszynski, *Growth factors and combinatorial therapies for CNS regeneration.* Experimental Neurology, 2008. **209**(2): p. 313-320.
68. Schwab, M.E., et al., *NERVE GROWTH-FACTOR (NGF) IN THE RAT CNS - ABSENCE OF SPECIFIC RETROGRADE AXONAL-TRANSPORT AND TYROSINE-HYDROXYLASE INDUCTION IN LOCUS COERULEUS AND SUBSTANTIA NIGRA.* Brain Research, 1979. **168**(3): p. 473-483.
69. Tuszynski, M.H., et al., *FIBROBLASTS GENETICALLY-MODIFIED TO PRODUCE NERVE GROWTH-FACTOR INDUCE ROBUST NEURITIC INGROWTH AFTER GRAFTING TO THE SPINAL-CORD.* Experimental Neurology, 1994. **126**(1): p. 1-14.

70. Grill, R., et al., *Cellular delivery of neurotrophin-3 promotes corticospinal axonal growth and partial functional recovery after spinal cord injury.* Journal of Neuroscience, 1997. **17**(14): p. 5560-5572.
71. Kobayashi, N.R., et al., *BDNF and NT-4/5 prevent atrophy of rat rubrospinal neurons after cervical axotomy, stimulate GAP-43 and T alpha 1-tubulin mRNA expression, and promote axonal regeneration.* Journal of Neuroscience, 1997. **17**(24): p. 9583-9595.
72. Cheng, H., Y.H. Cao, and L. Olson, *Spinal cord repair in adult paraplegic rats: Partial restoration of hind limb function.* Science, 1996. **273**(5274): p. 510-513.
73. Conner, J.M. and M.H. Tuszynski, *Growth factor therapy.* Mental Retardation and Developmental Disabilities Research Reviews, 1998. **4**(3): p. 212-222.
74. Lu, P., et al., *Combinatorial therapy with Neurotrophins and cAMP promotes axonal regeneration beyond sites of spinal cord injury.* Journal of Neuroscience, 2004. **24**(28): p. 6402-6409.
75. Pearse, D.D., et al., *cAMP and Schwann cells promote axonal growth and functional recovery after spinal cord injury.* Nature Medicine, 2004. **10**(6): p. 610-616.
76. Houle, J.D., et al., *Combining an autologous peripheral nervous system "bridge" and matrix modification by chondroitinase allows robust, functional regeneration beyond a hemisection lesion of the adult rat spinal cord.* Journal of Neuroscience, 2006. **26**(28): p. 7405-7415.
77. Peppas, N.A., et al., *Hydrogels in pharmaceutical formulations.* European Journal of Pharmaceutics and Biopharmaceutics, 2000. **50**(1): p. 27-46.
78. Lee, S.H. and H. Shin, *Matrices and scaffolds for delivery of bioactive molecules in bone and cartilage tissue engineering.* Advanced Drug Delivery Reviews, 2007. **59**(4-5): p. 339-359.
79. Peppas, N.A. and A.G. Mikos, *Preparation methods and structure of hydrogels.* Hydrogels in medicine and pharmacy, 1986. **1**: p. 1-27.
80. Brannon-Peppas, L., *Preparation and characterization of crosslinked hydrophilic networks.* Absorbent Polymer Technology, Studies in Polymer Sci, 1990. **8**: p. 45-66.
81. Lin, C.C. and A.T. Metters, *Hydrogels in controlled release formulations: Network design and mathematical modeling.* Advanced Drug Delivery Reviews, 2006. **58**(12-13): p. 1379-1408.
82. Peppas, N.A. and E.W. Merrill, *DIFFERENTIAL SCANNING CALORIMETRY OF CRYSTALLIZED PVA HYDROGELS.* Journal of Applied Polymer Science, 1976. **20**(6): p. 1457-1465.
83. Peppas, N.A. and N.K. Mongia, *Ultrapure poly(vinyl alcohol) hydrogels with mucoadhesive drug delivery characteristics.* European Journal of Pharmaceutics and Biopharmaceutics, 1997. **43**(1): p. 51-58.
84. Van Vlierberghe, S., et al., *Toward modulating the architecture of hydrogel scaffolds: curtains versus channels.* Journal of Materials Science-Materials in Medicine, 2008. **19**(4): p. 1459-1466.
85. Ratner, B.D. and A.S. Hoffman, *SYNTHETIC HYDROGELS FOR BIOMEDICAL APPLICATIONS.* Acs Symposium Series, 1976(31): p. 1-36.

86. Peppas, N.A., *Hydrogels and drug delivery.* Current Opinion in Colloid & Interface Science, 1997. **2**(5): p. 531-537.
87. Hamidi, M., A. Azadi, and P. Rafiei, *Hydrogel nanoparticles in drug delivery.* Advanced Drug Delivery Reviews, 2008. **60**(15): p. 1638-1649.
88. Gulrez, S.K., S. Al-Assaf, and G.O. Phillips, *Hydrogels: methods of preparation, characterisation and applications.* Progress in molecular and environmental bioengineering—from analysis and modeling to technology applications. InTech, Winchester, 2011: p. 117-150.
89. Lee, K.Y. and D.J. Mooney, *Hydrogels for tissue engineering.* Chemical Reviews, 2001. **101**(7): p. 1869-1879.
90. Luo, W., et al., *Synthesis and properties of starch grafted poly acrylamide-co-(acrylic acid) /montmorillonite nanosuperabsorbent via gamma-ray irradiation technique.* Journal of Applied Polymer Science, 2005. **96**(4): p. 1341-1346.
91. Huang, S. and D.E. Ingber, *The structural and mechanical complexity of cell-growth control.* Nature Cell Biology, 1999. **1**(5): p. E131-E138.
92. Lee, K.Y., et al., *Controlling mechanical and swelling properties of alginate hydrogels independently by cross-linker type and cross-linking density.* Macromolecules, 2000. **33**(11): p. 4291-4294.
93. Lee, K.Y., K.H. Bouhadir, and D.J. Mooney, *Degradation behavior of covalently cross-linked poly(aldehyde guluronate) hydrogels.* Macromolecules, 2000. **33**(1): p. 97-101.
94. Lopergolo, L.C., A.B. Lugao, and L.H. Catalani, *Direct UV photocrosslinking of poly(N-vinyl-2-pyrrolidone) (PVP) to produce hydrogels.* Polymer, 2003. **44**(20): p. 6217-6222.
95. Sperinde, J.J. and L.G. Griffith, *Control and prediction of gelation kinetics in enzymatically cross-linked poly(ethylene glycol) hydrogels.* Macromolecules, 2000. **33**(15): p. 5476-5480.
96. Pulapura, S. and J. Kohn, *Trends in the development of bioresorbable polymers for medical applications.* Journal of biomaterials applications, 1992. **6**(3): p. 216-250.
97. Parenteau-Bareil, R., R. Gauvin, and F. Berthod, *Collagen-Based Biomaterials for Tissue Engineering Applications.* Materials, 2010. **3**(3): p. 1863-1887.
98. Auger, F.A., et al., *Tissue-engineered human skin substitutes developed from collagen-populated hydrated gels: clinical and fundamental applications.* Medical & Biological Engineering & Computing, 1998. **36**(6): p. 801-812.
99. Laurent, T.C., U.B.G. Laurent, and J.R.E. Fraser, *FUNCTIONS OF HYALURONAN.* Annals of the Rheumatic Diseases, 1995. **54**(5): p. 429-432.
100. Fraser, J.R.E., T.C. Laurent, and U.B.G. Laurent, *Hyaluronan: Its nature, distribution, functions and turnover.* Journal of Internal Medicine, 1997. **242**(1): p. 27-33.
101. Van Vlierberghe, S., P. Dubruel, and E. Schacht, *Biopolymer-Based Hydrogels As Scaffolds for Tissue Engineering Applications: A Review.* Biomacromolecules, 2011. **12**(5): p. 1387-1408.
102. Turley, E.A., P.W. Noble, and L.Y.W. Bourguignon, *Signaling properties of hyaluronan receptors.* Journal of Biological Chemistry, 2002. **277**(7): p. 4589-4592.

103. Benedetti, L., et al., *BIOCOMPATIBILITY AND BIODEGRADATION OF DIFFERENT HYALURONAN DERIVATIVES (HYAFF) IMPLANTED IN RATS.* Biomaterials, 1993. **14**(15): p. 1154-1160.
104. Luo, Y., M.R. Ziebell, and G.D. Prestwich, *A hyaluronic acid-taxol antitumor bioconjugate targeted to cancer cells.* Biomacromolecules, 2000. **1**(2): p. 208-218.
105. Kuo, J.W., D.A. Swann, and G.D. Prestwich, *CHEMICAL MODIFICATION OF HYALURONIC-ACID BY CARBODIIMIDES.* Bioconjugate Chemistry, 1991. **2**(4): p. 232-241.
106. Hollinger, J.O., *An Introduction to Biomaterials*. 2005: CRC Press.
107. Augst, A.D., H.J. Kong, and D.J. Mooney, *Alginate hydrogels as biomaterials.* Macromolecular Bioscience, 2006. **6**(8): p. 623-633.
108. Gombotz, W.R. and S.F. Wee, *Protein release from alginate matrices.* Advanced Drug Delivery Reviews, 1998. **31**(3): p. 267-285.
109. Freeman, I. and S. Cohen, *The influence of the sequential delivery of angiogenic factors from affinity-binding alginate scaffolds on vascularization.* Biomaterials, 2009. **30**(11): p. 2122-2131.
110. Alshamkhani, A. and R. Duncan, *RADIOIODINATION OF ALGINATE VIA COVALENTLY-BOUND TYROSINAMIDE ALLOWS MONITORING OF ITS FATE IN-VIVO.* Journal of Bioactive and Compatible Polymers, 1995. **10**(1): p. 4-13.
111. Bouhadir, K.H., D.S. Hausman, and D.J. Mooney, *Synthesis of cross-linked poly(aldehyde guluronate) hydrogels.* Polymer, 1999. **40**(12): p. 3575-3584.
112. Jayakumar, R., et al., *Novel carboxymethyl derivatives of chitin and chitosan materials and their biomedical applications.* Progress in Materials Science, 2010. **55**(7): p. 675-709.
113. Van Vlierberghe, S., P. Dubruel, and E. Schacht, *Biopolymer-based hydrogels as scaffolds for tissue engineering applications: a review.* Biomacromolecules, 2011. **12**(5): p. 1387-408.
114. Kurita, K., et al., *Synthesis and some properties of nonnatural amino polysaccharides: Branched chitin and chitosan.* Macromolecules, 2000. **33**(13): p. 4711-4716.
115. Chenite, A., et al., *Novel injectable neutral solutions of chitosan form biodegradable gels in situ.* Biomaterials, 2000. **21**(21): p. 2155-2161.
116. Hoffmann, B., et al., *Glutaraldehyde and oxidised dextran as crosslinker reagents for chitosan-based scaffolds for cartilage tissue engineering.* Journal of Materials Science-Materials in Medicine, 2009. **20**(7): p. 1495-1503.
117. Heinemann, C., et al., *In Vitro Evaluation of Textile Chitosan Scaffolds for Tissue Engineering using Human Bone Marrow Stromal Cells.* Biomacromolecules, 2009. **10**(5): p. 1305-1310.
118. Nagahama, H., et al., *Preparation and characterization of novel chitosan/gelatin membranes using chitosan hydrogel.* Carbohydrate Polymers, 2009. **76**(2): p. 255-260.
119. Hong, H., C.S. Liu, and W.J. Wu, *Preparation and Characterization of Chitosan/PEG/Gelatin Composites for Tissue Engineering.* Journal of Applied Polymer Science, 2009. **114**(2): p. 1220-1225.

120. Thein-Han, W.W. and R.D.K. Misra, *Biomimetic chitosan-nanohydroxyapatite composite scaffolds for bone tissue engineering.* Acta Biomaterialia, 2009. **5**(4): p. 1182-1197.
121. Cai, X., et al., *Preparation and characterization of homogeneous chitosan-polylactic acid/hydroxyapatite nanocomposite for bone tissue engineering and evaluation of its mechanical properties.* Acta Biomaterialia, 2009. **5**(7): p. 2693-2703.
122. Zhu, C., et al., *Initial investigation of novel human-like collagen/chitosan scaffold for vascular tissue engineering.* Journal of Biomedical Materials Research Part A, 2009. **89A**(3): p. 829-840.
123. Gumbiner, B.M., *Cell adhesion: The molecular basis of tissue architecture and morphogenesis.* Cell, 1996. **84**(3): p. 345-357.
124. Hynes, R.O., *Integrins: a family of cell surface receptors.* Cell, 1987. **48**(4): p. 549-554.
125. Hersel, U., C. Dahmen, and H. Kessler, *RGD modified polymers: biomaterials for stimulated cell adhesion and beyond.* Biomaterials, 2003. **24**(24): p. 4385-4415.
126. Elbert, D.L. and J.A. Hubbell, *Conjugate addition reactions combined with free-radical cross-linking for the design of materials for tissue engineering.* Biomacromolecules, 2001. **2**(2): p. 430-441.
127. Boxus, T., et al., *Synthesis and evaluation of RGD peptidomimetics aimed at surface bioderivatization of polymer substrates.* Bioorganic & Medicinal Chemistry, 1998. **6**(9): p. 1577-1595.
128. Massia, S.P. and J.A. Hubbell, *AN RGD SPACING OF 440NM IS SUFFICIENT FOR INTEGRIN ALPHA-V-BETA-3-MEDIATED FIBROBLAST SPREADING AND 140NM FOR FOCAL CONTACT AND STRESS FIBER FORMATION.* Journal of Cell Biology, 1991. **114**(5): p. 1089-1100.
129. Hubbell, J.A., *Bioactive biomaterials.* Current Opinion in Biotechnology, 1999. **10**(2): p. 123-129.
130. Drumheller, P.D. and J.A. Hubbell, *POLYMER NETWORKS WITH GRAFTED CELL-ADHESION PEPTIDES FOR HIGHLY BIOSPECIFIC CELL ADHESIVE SUBSTRATES.* Analytical Biochemistry, 1994. **222**(2): p. 380-388.
131. Dai, W.G., J. Belt, and W.M. Saltzman, *CELL-BINDING PEPTIDES CONJUGATED TO POLY(ETHYLENE GLYCOL) PROMOTE NEURAL CELL-AGGREGATION.* Bio-Technology, 1994. **12**(8): p. 797-801.
132. Borkenhagen, M., et al., *Three-dimensional extracellular matrix engineering in the nervous system.* Journal of Biomedical Materials Research, 1998. **40**(3): p. 392-400.
133. Nomizu, M., et al., *STRUCTURE-ACTIVITY STUDY OF A LAMININ ALPHA-1 CHAIN ACTIVE PEPTIDE SEGMENT ILE-LYS-VAL-ALA-VAL (IKVAV).* Febs Letters, 1995. **365**(2-3): p. 227-231.
134. Burmeister Getz, E., et al., *A comparison between the sulfhydryl reductants tris(2-carboxyethyl)phosphine and dithiothreitol for use in protein biochemistry.* Analytical Biochemistry, 1999. **273**(1): p. 73-80.
135. Lambeth, D.O., et al., *IMPLICATIONS FOR INVITRO STUDIES OF THE AUTOXIDATION OF FERROUS ION AND THE IRON-CATALYZED AUTOXIDATION*

OF DITHIOTHREITOL. Biochimica Et Biophysica Acta, 1982. **719**(3): p. 501-508.
136. Bagiyan, G.A., et al., *Oxidation of thiol compounds by molecular oxygen in aqueous solutions.* Russian Chemical Bulletin, 2003. **52**(5): p. 1135-1141.
137. Riddles, P.W., R.L. Blakeley, and B. Zerner, *ELLMANS REAGENT - 5,5'-DITHIOBIS(2-NITROBENZOIC ACID) - RE-EXAMINATION.* Analytical Biochemistry, 1979. **94**(1): p. 75-81.
138. Staros, J.V., R.W. Wright, and D.M. Swingle, *ENHANCEMENT BY N-HYDROXYSULFOSUCCINIMIDE OF WATER-SOLUBLE CARBODIIMIDE-MEDIATED COUPLING REACTIONS.* Analytical Biochemistry, 1986. **156**(1): p. 220-222.
139. Nyquist, R.A. and W.J. Potts, *CHARACTERISTIC INFRARED ABSORPTION FREQUENCIES OF THIOL ESTERS AND RELATED COMPOUNDS.* Spectrochimica Acta, 1959. **15**(7): p. 514-538.
140. Shu, X.Z., et al., *Disulfide-crosslinked hyaluronan-gelatin hydrogel films: a covalent mimic of the extracellular matrix for in vitro cell growth.* Biomaterials, 2003. **24**(21): p. 3825-3834.
141. Luo, Y. and G.D. Prestwich, *Hyaluronic acid-N-hydroxysuccinimide: A useful intermediate for bioconjugation.* Bioconjugate Chemistry, 2001. **12**(6): p. 1085-1088.
142. Singh, R. and G.M. Whitesides, *A REAGENT FOR REDUCTION OF DISULFIDE BONDS IN PROTEINS THAT REDUCES DISULFIDE BONDS FASTER THAN DOES DITHIOTHREITOL.* Journal of Organic Chemistry, 1991. **56**(7): p. 2332-2337.
143. Krepela, E., J. Prochazka, and B. Karova, *Regulation of cathepsin B activity by cysteine and related thiols.* Biological Chemistry, 1999. **380**(5): p. 541-551.
144. Gu, C.F., D.Y. Chen, and M. Jiang, *Short-life core-shell structured nanoaggregates formed by the self-assembly of PEO-b-PAA/ETC (1-(3-dimethylaminopropyl)-3-ethylcarbodiimide methiodide) and their stabilization.* Macromolecules, 2004. **37**(4): p. 1666-1669.
145. Benesova, K., et al., *Stability evaluation of n-alkyl hyaluronic acid derivates by DSC and TG measurement.* Journal Of Thermal Analysis And Calorimetry, 2006. **83**(2): p. 341-348.
146. Villetti, M.A., et al., *Thermal degradation of natural polymers.* Journal of Thermal Analysis and Calorimetry, 2002. **67**(2): p. 295-303.
147. Tokita, Y., K. Ohshima, and A. Okamoto, *Degradation of hyaluronic acid during freeze drying.* Polymer Degradation and Stability, 1997. **55**(2): p. 159-164.
148. Serban, M.A., G. Yang, and G.D. Prestwich, *Synthesis, characterization and chondroprotective properties of a hyaluronan thioethyl ether derivative.* Biomaterials, 2008. **29**(10): p. 1388-99.
149. Hu, B.H., J. Su, and P.B. Messersmith, *Hydrogels Cross-Linked by Native Chemical Ligation.* Biomacromolecules, 2009. **10**(8): p. 2194-2200.
150. Wu, Z.M., et al., *Disulfide-crosslinked chitosan hydrogel for cell viability and controlled protein release.* European Journal of Pharmaceutical Sciences, 2009. **37**(3-4): p. 198-206.

151. Smyth, D.G., W. Konigsberg, and O.O. Blumenfeld, *REACTIONS OF N-ETHYLMALEIMIDE WITH PEPTIDES + AMINO ACIDS.* Biochemical Journal, 1964. **91**(3): p. 589-&.
152. Khetan, S. and J.A. Burdick, *Patterning network structure to spatially control cellular remodeling and stem cell fate within 3-dimensional hydrogels.* Biomaterials, 2010. **31**(32): p. 8228-8234.
153. Censi, R., et al., *In Situ Forming Hydrogels by Tandem Thermal Gelling and Michael Addition Reaction between Thermosensitive Triblock Copolymers and Thiolated Hyaluronan.* Macromolecules, 2010. **43**(13): p. 5771-5778.
154. Deng, C., et al., *A Collagen-Chitosan Hydrogel for Endothelial Differentiation and Angiogenesis.* Tissue Engineering Part A, 2010. **16**(10): p. 3099-3109.
155. Matsuda, T., et al., *Photoinduced prevention of tissue adhesion.* ASAIO journal, 1992. **38**(3): p. M154-M157.
156. Duranti, F., et al., *Injectable hyaluronic acid gel for soft tissue augmentation - A clinical and histological study.* Dermatologic Surgery, 1998. **24**(12): p. 1317-1325.
157. Galassi, G., et al., *In vitro reconstructed dermis implanted in human wounds: degradation studies of the HA-based supporting scaffold.* Biomaterials, 2000. **21**(21): p. 2183-2191.
158. Maaser, K., et al., *Functional hierarchy of simultaneously expressed adhesion receptors: Integrin alpha 2 beta 1 but not CD44 mediates MV3 melanoma cell migration and matrix reorganization within three-dimensional hyaluronan-containing collagen matrices.* Molecular Biology of the Cell, 1999. **10**(10): p. 3067-3079.
159. Horn, E.M., et al., *Influence of cross-linked hyaluronic acid hydrogels on neurite outgrowth and recovery from spinal cord injury.* Journal Of Neurosurgery-Spine, 2007. **6**(2): p. 133-140.
160. de Ruiter, G.C.W., et al., *Nerve Tubes for Peripheral Nerve Repair.* Neurosurgery Clinics of North America, 2009. **20**(1): p. 91-+.
161. Ruiter, G.C.W., et al., *Designing ideal conduits for peripheral nerve repair.* Neurosurgical Focus, 2009. **26**(2).